Title: Ligand-receptor co-evolution shaped the jasmonate pathway in land plants.

Authors: Monte I, Ishida S, Zamarreño AM, Hamberg M, Franco-Zorrilla JM, García-Casado G, Gouhier-Darimont C, Reymond P, Takahashi K, García-Mina JM, Nishihama R, Kohchi T, Solano R

Journal: Nature chemical biology

Year: 2018 May

Issue: 14

Volume: 5

Pages: 480-488

DOI: 10.1038/s41589-018-0033-4

Ligand-receptor co-evolution shaped the jasmonate pathway in land plants

Isabel Monte[1], Sakiko Ishida[2], Angel M. Zamarreño[3], Mats Hamberg[4], José M. Franco-Zorrilla[5], Gloria García-Casado[5], Caroline Gouhier-Darimont[6], Philippe Reymond[6], Kosaku Takahashi[7], José M. García-Mina[3], Ryuichi Nishihama[2], Takayuki Kohchi[2] and Roberto Solano[1]*

[1] Department of Plant Molecular Genetics, Centro Nacional de Biotecnología, Consejo Superior de Investigaciones Científicas (CNB-CSIC), 28049 Madrid, Spain

[2] Graduate School of Biostudies, Kyoto University, Kyoto 606-8502, Japan

[3] Environmental Biology Department, University of Navarra, Navarre, Spain

[4] Division of Physiological Chemistry II, Department of Medical Biochemistry and Biophysics, Karolinska Institutet, Stockholm, Sweden

[5] Genomics Unit, Centro Nacional de Biotecnología, Consejo Superior de Investigaciones Científicas (CNB-CSIC), 28049 Madrid, Spain

[6] Department of Plant Molecular Biology, University of Lausanne, CH-1015 Lausanne, Switzerland

[7] Research Faculty of Agriculture, Division of Applied Bioscience, Hokkaido University, Sapporo, Japan

*Corresponding author: rsolano@cnb.csic.es

SUMMARY

The phytohormone jasmonoyl-isoleucine (JA-Ile) regulates defence, growth and developmental responses in vascular plants. Bryophytes have conserved sequences for all JA-Ile signalling pathway components but lack JA-Ile. We show that, in spite of 450 million years of independent evolution, the JA-Ile receptor COI1 is functionally conserved between the bryophyte *Marchantia polymorpha* and the eudicot *Arabidopsis thaliana*, but COI1 responds to different ligands in each species. We identified the ligand of Marchantia MpCOI1 as two isomeric forms of the JA-Ile precursor dinor-OPDA (dinor-*cis*-OPDA and dinor-*iso*-OPDA). We demonstrate that AtCOI1 functionally complements Mp*coi1* mutation and confers JA-Ile responsiveness, and that a single residue substitution in MpCOI1 is responsible for the evolutionary switch in ligand specificity. Our results identify the ancestral bioactive jasmonate, clarify its biosynthetic pathway, demonstrate the functional conservation of its signalling pathway, and show that JA-Ile and COI1 emergence in vascular plants required co-evolution of hormone biosynthetic complexity and receptor specificity.

250 character summary

The bioactive jasmonate in bryophytes is not known. Here we demonstrate that the JA-Ile receptor COI1 is functionally conserved among land plants and identify the COI1 ligand in bryophytes as two isomers of the JA-Ile precursor dinor-OPDA.

Jasmonoyl-isoleucine (JA-Ile; **1**), a fatty acid-derived phytohormone chemically similar to animal prostaglandins, regulates activation of responses to many biotic and abiotic stresses in vascular plants. JA-Ile is also an essential regulator of many physiological and developmental processes[1–3].

Hormone synthesis starts in chloroplasts by lipase-mediated release of the membrane fatty acids α-linolenic or hexadecatrienoic acids[2]. Oxygenation by 13-lipoxygenases and dehydration-cyclization by the enzymes AOS and AOC lead to 12-oxo-phytodienoic acid (OPDA; **2**) production. OPDA is transported into the peroxisome, where it is reduced by OPDA-reductase 3 (OPR3) and undergoes three β-oxidation cycles to produce jasmonic acid (JA; **3**). Cytoplasmic JAR1 (Jasmonate-amido synthetase 1) conjugates JA to Ile, giving rise to the bioactive hormone, (+)-7-*iso*-JA-L-Ile[4,5]. This biosynthetic pathway is widely conserved in tracheophytes and has been recently characterized in *Selaginella moellendorffii* where JA-Ile has been detected[2,6,7].

JA-Ile triggers interaction between the receptor F-box protein COI1 and members of the JAZ (jasmonate-ZIM domain) family of repressors, which are also hormone co-receptors[8–12]. COI1-mediated degradation of JAZ repressors is the key step to derepress transcription factors and activate genetic reprograming of the cell in response to the hormone [3,9,10,13,14].

Arabidopsis thaliana has been an instrumental model system in identifying the bioactive hormone and elucidating its signal transduction pathway in eudicots. Nonetheless, *A. thaliana* is just one of the ~400,000 plant species on earth, many of them separated by millions of years of evolution. Detailed knowledge of the Arabidopsis JA-Ile signalling pathway is thus unlikely to represent its diversity in other plant lineages. Current genome sequencing projects have been instrumental in identifying candidate orthologue genes in diverse organisms. However, candidate orthologue gene identification is just a first step towards unveiling mechanistic specificities shaped by evolution. For instance, genome sequences for all bryophyte lineages (hornworts, liverworts, and mosses)[15–18] show conserved gene candidates for all core components of the JA-Ile signalling pathway, COI1, JAZ, MYC, NINJA and TPL. Recent genome analysis of the liverwort *Marchantia polymorpha* showed that this pathway first appeared in the common ancestor of extant land plants more than 450

million years ago[18]. However, bryophyte capacity to synthesize and/or respond to JA-Ile is debated. Whereas JA and JA-Ile accumulation was reported in liverworts and mosses[19–21], orthologues of key enzymes for JA and JA-Ile biosynthesis appear to be absent in the *M. polymorpha* and *Physcomitrella patens* genomes[15,18]. Experimental evidence supports the idea that *P. patens* and *M. polymorpha* can synthesize the JA precursor OPDA, but due to lack of OPR3 and JAR1, they cannot produce JA-Ile[22–25]. This is consistent with the proposed first appearance of OPR3 and JAR1 functions and JA-Ile in lycophytes[7]. Bryophytes thus have putative conserved JA-Ile signalling machinery but lack JA-Ile, which suggests the use of a distinct signalling molecule.

Here we addressed the functional conservation of the COI1 receptor in bryophytes and the identification of its ligand in the liverwort *M. polymorpha*. This model plant has a relatively small genome and a privileged phylogenetic position. Although the order of bryophyte evolutionary divergence is still not unequivocally resolved[26], liverworts have been proposed to be the sister lineage of all other land plants based on genome analysis and fossil records[18]. Therefore, Marchantia is a unique model for evolutionary studies since conserved features with other plants should be already present in the common ancestor of land plants that conquer the land more than 450 million years ago. Besides evolutionary importance, Marchantia is revolutionizing our way to approach biological questions in plants due to its unprecedentedly low gene redundancy, which might help uncover regulatory mechanisms hidden by gene redundancy in later-diverged plants[18]. Using a combination of molecular genetics and biochemical (metabolite analysis) approaches, we show that COI1 is functionally conserved in land plant evolution (at least between *M. polymorpha* and *A. thaliana*) but responds to different ligands, which we identified as two isomeric forms of the JA-Ile precursor dinor-OPDA in *M. polymorpha*. We demonstrate that a single residue substitution in COI1 is responsible for the evolutionary switch in ligand specificity. These

results identify the jasmonate hormone in bryophytes and explain the evolutionary events that led JA-Ile and COI1 to emerge in vascular plants from their ancestral counterparts.

RESULTS

M. polymorpha neither synthesizes nor perceives JA-Ile

The reported wound-induced accumulation of OPDA in *M. polymorpha* is very late (8 h post-stimulation), which questions its function as a signalling molecule[24]. To test whether *M. polymorpha* can produce JA-Ile and to characterize OPDA accumulation kinetics, we measured OPDA, JA and JA-Ile levels in WT male (Tak-1) plants after stimulation by wounding (**Supplementary Fig. 1a**). As in vascular plants, wounding induced rapid (5 min), transient OPDA accumulation, which decreased 1 h post-stimulation[27]. JA-Ile was not detected in these plants, and only residual amounts of JA, near the detection limit, were measured (**Supplementary Fig. 1b**). This is consistent with the fact that the two GH3-like enzymes in *M. polymorpha* are less related phylogenetically to JAR1 than those in *P. patens*, which are involved in auxin conjugation (**Supplementary Fig. 1c**)[22]. It is also consistent with the phylogenetic proximity of the two *M. polymorpha* OPR-like enzymes to OPR1 and OPR2, rather than to OPR3 (**Supplementary Fig. 1c**). These results indicate that if the pathway is functionally conserved, the hormone that activates it in bryophytes must differ from JA-Ile.

In vascular plants, JA-Ile and its precursors JA and OPDA inhibit growth[28] (**Supplementary Fig. 1d,e**). Exogenous treatment of *M. polymorpha* Tak-1 plants with OPDA also inhibited growth (**Supplementary Fig. 1f,g**), whereas these plants were completely insensitive to JA and JA-Ile, which indicated that JA-Ile is neither produced nor perceived in *M. polymorpha*. Similar growth-inhibitory effects of OPDA, but not of JA or JA-Ile, were observed in *P. patens* and the hornwort *Anthoceros agrestis* (**Supplementary Fig. 1f,g**). These results show that in bryophytes, the hormone that activates this pathway is

potentially related to OPDA but not to JA or JA-Ile, as bryophytes do not synthesize nor detect JA or JA-Ile.

Identification of the Marchantia AtCOI1 orthologue

The finding of COI1- and JAZ-related sequences in the *M. polymorpha* genome suggests a conserved hormone receptor machinery in land plant evolution[18]. To examine whether there is functional conservation of the jasmonate signalling pathway in a plant that lacks JA-Ile, we generated knock-out mutant alleles in the male (Tak-1) and the female (Tak-2) backgrounds for the Marchantia gene closest to At*COI1*, Mapoly0025s0025 (Mp*COI1*), using homologous recombination-mediated gene targeting (Mp*coi1-1*)[29,30] and CRISPR/Cas9^{D10A} technology (Mp*coi1-2* and Mp*coi1-3*; **Supplementary Fig. 2a,b**)[31–34]. The closest gene to Mapoly0025s0025 in the Marchantia genome encodes for an AtTIR1 orthologue[18], suggesting that MpCOI1 function is encoded by a single gene with no redundancy. All three Mp*coi1* alleles were insensitive to OPDA-triggered growth inhibition independently of the sex of the plant (**Fig. 1a,b**), and this phenotype could be reversed by complementation with the WT *MpCOI1* gene (**Fig. 1c,d**). These data indicate that MpCOI1 is the functional orthologue of the AtCOI1 receptor in *M. polymorpha* and that, similar to angiosperms, the MpCOI1-dependent pathway controls growth in response to OPDA.

Besides growth, the COI1 pathway regulates jasmonate biosynthesis, plant defence and fertility in Arabidopsis[2]. Liquid chromatography-mass spectrometry (LC-MS) quantification of OPDA levels showed that Mp*coi1-1* has approximately one third of OPDA produced by WT (Tak-1) in basal conditions (**Fig. 1e**), which suggests that the COI1-dependent positive feedback loop that regulates this biosynthetic pathway in Arabidopsis is also found in Marchantia[2].

To determine whether the MpCOI1 pathway regulates defence responses in *M. polymorpha* as it does in eudicots, we challenged Mp*coi1-1* and wild-type thalli with larvae

from the generalist herbivore *Spodoptera littoralis*. Larvae fed on the Mp*coi1-1* mutant weighed twice as much as those that fed on wild-type WT Tak-1 or Tak-2 (**Fig. 1f**), indicating that MpCOI1 is necessary for defence against the insect in *M. polymorpha*, and that the role of this signalling pathway in plant defence is thus also conserved in land plants.

Fertility is compromised in Arabidopsis mutants with altered JA-Ile biosynthesis, such as *aos1*[35], or perception, such as *coi1*[8,36]. OPDA biosynthetic *P. patens* mutants also show reduced fertility[23]. In contrast, Mp*coi1* female and male mutants were crossed successfully and backcrossed to wild-type. The sporangia showed no developmental defects and the mutation segregated as expected (1:1; **Supplementary Fig. 2c,d**). Fertility is therefore not an ancient character regulated by the COI1 pathway, which was likely co-opted more recently in evolution.

To examine the extent of evolutionary conservation of COI1 function, we attempted to complement Mp*coi1-1* by expressing Arabidopsis At*COI1* in transgenic Marchantia plants. In spite of more than 450 million years of independent evolution and the lack of JA-Ile in Marchantia, expression of At*COI1* using two distinct constitutive promoters (Mp*EF1* and CaMV 35S) restored partial OPDA responsiveness (**Fig. 2a,b**). This suggests that AtCOI1 remains able to perceive the bryophyte hormone, although with lower affinity than MpCOI1. In contrast to WT plants, transgenic Mp*coi1* mutants expressing AtCOI1 ($_{pro}$Mp*EF1*:At*COI1*/Mp*coi1-1* and 35S:At*COI1*/Mp*coi1-1*) remarkably perceived JA-Ile and its mimic coronatine (COR; **4**; a bacterially produced COI1 ligand; **Fig. 2a,b**)[37]. These data confirm the functional correspondence between MpCOI1 and AtCOI1, and unveil their differences in ligand specificity. In addition, the results indicate the large extent of conservation of the entire signalling pathway, since AtCOI1 recapitulates all events that lead to growth inhibition in response to molecules that do not act on WT Marchantia.

To examine conservation at the molecular level, we designed a microarray of the Marchantia genome (see Methods). Transcriptomic analyses[38] showed that most genes upregulated by OPDA treatment were also upregulated by wounding (**Fig. 3a,b; Supplementary Dataset 1**), which indicated that as in the JA-Ile pathway in vascular plants[2,39], OPDA regulates wounding responses in *M. polymorpha*. In Mp*coi1*, OPDA did not induce expression of most OPDA-upregulated genes in the WT (**Fig. 3b, Supplementary Dataset 1 and Supplementary Fig. 3a**). COR treatment mimicked OPDA responsiveness in complemented Mp*coi1* mutants that expressed AtCOI1 ($_{pro}$Mp*EF1*:At*COI1*/Mp*coi1-1*), which further confirmed functional conservation of COI1 (**Fig. 3b; Supplementary Dataset 1**). Q-PCR analysis of marker genes confirmed their MpCOI1-dependent or independent induction by OPDA and the complementation by AtCOI1 (**Supplementary Fig. 3a**). Gene ontology (GO) analysis of the MpCOI1-dependent clusters using the Marchantia annotation or that of Arabidopsis homologues indicated enrichment of jasmonate-, wounding-, defence and lipid metabolism-related processes, further substantiating functional conservation (**Supplementary Dataset 2 and 3**).

The G-box (CACGTG) is the target of AtCOI1-regulated AtMYC transcription factors[9,40]. We detected significant enrichment of this box in the proximal promoter region of OPDA- or wounding-upregulated genes compared to its presence in the Marchantia genome (**Supplementary Fig. 3b,c**). This suggests that MYC function is also conserved downstream of hormone perception.

Val^{377} in MpCOI1 determines ligand specificity

To identify the COI1 protein residues that determine ligand specificity, we examined the *in vivo* function of chimaeric proteins that combine the N-terminal half of AtCOI1 and C-terminal half of MpCOI1 (At*COI*-Mp*COI*) or vice versa (Mp*COI*-At*COI*). Both chimaera types complemented the Mp*coi1* response to OPDA (**Fig. 4a,b**). Nonetheless, only plants

bearing the C-terminal part of AtCOI1 responded to JA-Ile like plants that express full-length AtCOI1. The hormone specificity determinants are therefore located in the C terminus.

Alignments of available sequences of the C-terminal half of COI1 from several species[16,41] showed a striking difference between bryophyte and tracheophyte sequences at AtCOI1 position 384 (377 in MpCOI1). All vascular plants bear an alanine in this position, whereas bryophytes predominantly show valine or isoleucine, but never Ala (**Fig. 4c and Supplementary Fig. 4**). Available structural data showed that AtCOI1 Ala384 contacts the isoleucine side chain of JA-Ile[11], which suggests that this difference between bryophytes and tracheophytes is important for ligand specification. We therefore mutated the Val in MpCOI1 to Ala and analysed the specificity of the resulting protein (MpCOI1^{V377A}). MpCOI1^{V377A} expression in the Mp*coi1-1* background restored OPDA sensitivity, indicating that the mutant protein MpCOI1^{V377A} is active and complements the Mp*coi1-1* mutation (**Fig. 4d,e**). Strikingly, the transgenic plants were also able to perceive both JA-Ile and COR (**Fig. 4d,e**), similar to plants expressing At*COI1* in Mp*coi1-1* (**Fig. 2**). A single amino acid change thus switches MpCOI1 ligand specificity to that of AtCOI1, which underlies the evolutionary divergence of the jasmonate ligand in early and late diverged plants.

The Val-to-Ala change enlarges the MpCOI1 pocket, allowing JA-Ile or COR binding (see below). Since the MpCOI1 hormone-binding pocket is smaller than that of vascular plants, it is likely that the bryophyte hormone would also be smaller than JA-Ile.

OPDA is a precursor of the MpCOI1 ligand

In Arabidopsis, AtCOI1 interacts with AtJAZ only in the presence of the hormone JA-Ile or its mimic, COR[5,11]. Since OPDA, but not JA or JA-Ile, accumulates after wounding in WT Marchantia plants, we tested whether OPDA is the MpCOI1/MpJAZ co-receptor ligand. We performed pull-down assays with OPDA, JA-Ile and COR, using AtCOI1/AtJAZ9 as a positive control. In contrast to JA-Ile or COR, OPDA did not induce the interaction between

AtCOI1 and AtJAZ9, as described[5] (**Supplementary Fig. 5a**). OPDA, JA-Ile or COR were unable to induce the MpCOI1/MpJAZ interaction (**Supplementary Fig. 5b**), which suggests that the active hormone that binds the MpCOI1/MpJAZ co-receptor is not OPDA, but possibly an OPDA derivative.

OPDA produces dn-OPDA isomers after wounding

To identify the OPDA-derived ligand of MpCOI1, we used LC-MS to measure OPDA-related compounds previously identified in plants, for which we had available standards or were able to synthesize (compounds in bold in **Supplementary Fig. 6**). In addition to OPDA, only 2,3-dinor-OPDA (dn-OPDA; **5**)[42] and to a higher level its isomer 2,3-dinor-12-oxo-9(13),15(*Z*)-phytodienoic acid (dn-*iso*-OPDA; **8**) accumulated in wounded plants, with kinetics similar to that of OPDA (**Fig. 5a**). In contrast to Marchantia, Arabidopsis plants were only able to synthesize dn-OPDA, but not dn-*iso*-OPDA (**Supplementary Fig. 7a**) suggesting the presence in Marchantia of a dn-OPDA $\Delta^{10} \rightarrow \Delta^{9(13)}$ isomerase activity. Consistent with this accumulation, in addition to OPDA only dinor-OPDA and dinor-*iso*-OPDA inhibited growth in an MpCOI1-dependent manner, while the other compounds tested produced no effect *in planta* (**Supplementary Fig. 7b**).

It has long been assumed that the major source of dinor-OPDA in angiosperms is hexadecatrienoic acid, which is also abundant in Marchantia chloroplast membranes[42,43]. Although conversion of OPDA into dn-OPDA and/or dn-*iso*-OPDA has not been reported yet in Marchantia, dn-OPDA synthesis from OPDA has been recently detected in Arabidopsis[44]. To test whether both hexadecatrienoic acid and OPDA can be dinor-OPDA precursors in Marchantia, we fed WT plants with deuterated OPDA (d5-OPDA), deuterated α-linolenic acid (d5-18:3; the OPDA precursor; **Supplementary Fig. 6**), or deuterated hexadecatrienoic acid (d6-16:3), and used LC-MS to quantify plant production of deuterated derivatives. Both d5-dn-OPDA isomers accumulated after d5-OPDA treatment (**Fig. 5b**), which indicated that

OPDA can be converted efficiently to dn-OPDA in Marchantia. The OPR3-mediated OPDA derivative OPC-6 was not detected, which confirmed lack of OPR3 activity in this plant. d5-OPDA and both d5-dn-OPDA isomers also accumulated after feeding plants with d5-18:3, which further supports the idea that OPDA is converted into dn-OPDA and dn-*iso*-OPDA in Marchantia (**Supplementary Fig. 8a,b**). Treatment with d6-16:3 resulted in rapid accumulation of both d5-dn-OPDA isomers, but not of d5-OPDA (**Supplementary Fig. 8c**). These data confirm that both hexadecatrienoic and linolenic acids are dn-OPDA sources (**Supplementary Fig. 6**). Non-deuterated OPDA and dn-OPDA isomers also accumulated after all three treatments with deuterated precursors, which indicates that synthesis of the hormone is subject to positive feedback, as is the case in angiosperms (**Supplementary Fig. 8d,e,f**)[2].

Dn-*iso*-OPDA and dn-*cis*-OPDA are MpCOI1 ligands

Although the *cis* and *trans* stereoisomers of dn-OPDA were not separated in our LC-MS assays, we prepared pure dn-*trans*-OPDA (**6**) and tested the activity of the three possible isomers, dn-*cis*-OPDA (**7**), dn-*trans*-OPDA and dn-*iso*-OPDA (**Fig. 6a**). Treatment of plants with similar concentrations of OPDA and dn-OPDA isomers showed that dn-*iso*-OPDA and dn-*cis*-OPDA have a greater inhibitory effect than OPDA in WT plants, and that this effect was completely MpCOI1-dependent (**Fig. 6b,c**). Dn-*trans*-OPDA was very poorly active compared to the *iso* and *cis* isomers, and we cannot discard that this activity is a consequence of *trans/cis* isomerization in the plant. To determine whether dn-*cis*-OPDA or dn-*iso*-OPDA are the bioactive hormone or yet other precursors, we used cell-free pull-down assays to test their capacity to trigger formation of the co-receptor MpCOI1/MpJAZ complex. Increasing dn-*cis*-OPDA and dn-*iso*-OPDA concentrations triggered retention by the immobilized MBP-MpJAZ protein of increasing amounts of MpCOI1 from plant cell-free extracts, whereas dn-*trans*-OPDA was almost inactive (**Fig. 6d**). Again, OPDA, JA-Ile and COR did not behave as

ligands of the MpCOI1/MpJAZ co-receptor (**Supplementary Fig. 9a**). To further support that these two isomers of dn-OPDA are the ligands of MpCOI1 we analyzed MpCOI1/MpJAZ interaction in a yeast heterologous system (yeast two-hybrid assays[45]) where other components of this signalling pathway are not conserved. As shown in **Figure 6e**, JA-Ile had no effect on yeast growth, further indicating that JA-Ile is not a ligand of MpCOI1. In contrast, both dn-*iso*-OPDA and dn-*cis*-OPDA promoted the interaction between MpCOI1 and MpJAZ and therefore yeast growth. This effect was clear even in the case of dn-*cis*-OPDA in spite of its toxicity for yeast cells that reduced growth of the positive control (**Fig. 6e**).

These results indicate that dn-*iso*-OPDA and, to a lesser extent, dn-*cis*-OPDA are the MpCOI1 ligands and, therefore, the bioactive jasmonates in *Marchantia polymorpha*.

Finally, since dn-*cis*-OPDA also accumulates in Arabidopsis (**Supplementary Fig. 7a**) and AtCOI1 partially complements the Mp*coi1* mutant, we tested whether dn-*cis*-OPDA and dn-*iso*-OPDA could be ligands of AtCOI1. As shown in **Figure 6f**, dn-*cis*-OPDA and, to a lesser extent dn-*iso*-OPDA promoted the interaction of AtCOI1 with MpJAZ. This result explains why AtCOI1 can complement the Mp*coi1* mutant and raises the interesting possibility that dn-OPDA could retain some of its hormonal function in vascular plants.

Finally, to mechanistically understand the wider ligand response conferred by the MpCOI1^{V377A} mutation in Marchantia we compared the binding capacity of this mutant protein to dn-OPDA and COR. **Supplementary Figure 9b** shows that COR can trigger the interaction of MpCOI1^{V377A} with MpJAZ similar to dn-*cis*-OPDA, further supporting that this particular amino acid has a key role in ligand specification and COI1 evolution.

Discussion

In this study, we identified a hormone, dn-OPDA, with two active isoforms in *Marchantia polymorpha*, and show that bryophytes and vascular plants share a conserved signalling machinery that is activated by distinct molecules (dn-*iso*-OPDA/dn-*cis*-OPDA or JA-Ile).

Understanding the evolution of land plants is a major issue in biology. Genome sequences available from a myriad of sequencing projects provide an unprecedented opportunity to study pathway conservation among plant lineages and to understand the degree to which the knowledge obtained in eudicot models represents plant diversity. More importantly, comparative genomics should help to identify mechanisms that might be hidden by the complexity of gene redundancy in late-derived plants.

Identification of candidate gene orthologues by sequencing programs may provide a first clue on the evolution of signalling pathways. However understanding the extent of conservation and divergence requires functional analyses. In this context, the liverwort *Marchantia polymorpha* is emerging as a model system for these types of studies. Although it is still a matter of debate[26], liverworts are considered the sister lineage to all other land plants[18] and therefore, Marchantia represents a unique model for evolutionary studies since conserved features with other plants should be already present in the common ancestor of land plants that conquer the land more than 450 million years ago[18]. Besides evolutionary importance, the presence in its genome of single copies for most of regulatory genes facilitates identification of orthologue candidates and their functional validation due to limited redundancy[18], which represents a major problem for gene discovery in later-evolved plants. In fact, we found that there is a single copy of each of the core components of the jasmonate pathway, which together with the functional conservation shown here indicate that this pathway appeared in the first common ancestor of extant land plants[18]. However, the hormones that activate the JA pathway must be different in bryophytes and vascular plants

since liverworts and mosses lack two key enzymes (OPR3 and JAR1) needed for the biosynthesis of JA-Ile, and would thus be unable to synthesize it (this study)[23,24]. Consistent with this hypothesis, we found that JA-Ile is neither synthesized nor perceived by bryophytes, but rather that Marchantia produces two isomers of dn-OPDA, *i.e.* dn-*cis*-OPDA and dn-*iso*-OPDA, as the bioactive ligands of its COI1 receptor. The wound-induced accumulation of OPDA and dn-OPDA isomers indicates that the chloroplastic steps of JA biosynthesis are conserved in bryophytes and vascular plants, and would therefore have been present in their common ancestor. In eudicots, the major sources of these compounds are α-linolenic (18:3) and hexadecatrienoic (16:3) acids[2]. These two fatty acids are abundant in Marchantia chloroplastic membranes[43]; however, the observation that OPDA inhibits growth in Marchantia plants coupled with the finding that only dn-OPDA isomers, and not OPDA, are MpCOI1 ligands suggested OPDA as an additional dn-OPDA source. Our results using deuterated α-linolenic and deuterated OPDA showed that this conversion takes place in Marchantia and clarifies the biosynthetic steps to the bioactive hormone form in this plant. OPDA conversion into dn-OPDA has been recently reported to occur also in Arabidopsis[44], which suggests that this is an ancient reaction, likely present in the ancestor of land plants. This ancient reaction likely gave rise to the JA-related hormone in bryophytes (dn-*cis*-OPDA and dn-*iso*-OPDA) and to the OPR3-independent pathway for JA biosynthesis described in vascular plants[44]. Therefore, OPR3 acquisition during evolution represents a more recent event that favoured JA production in vascular plants.

In spite of general functional conservation, not all processes regulated by COI1 in vascular plants are regulated by MpCOI1 in *M. polymorpha*. In eudicots, the COI1 pathway regulates three main physiological processes in the plant that can be summarized as plant growth, defence and fertility[2]. In *M. polymorpha*, MpCOI1 is also involved in two of these processes, defence and growth inhibition by OPDA/dn-OPDA, but does not regulate fertility. In fact,

Mp*coi1* female or male mutants were fully fertile in reciprocal crosses with WT or among them. Therefore, fertility is not an ancient character regulated by the COI1 pathway, and was likely co-opted more recently in evolution.

The discovery of the hormone (dn-*iso*-OPDA/dn-*cis*-OPDA) and the fact that a single amino acid in MpCOI1 switches ligand specificity to that of AtCOI1 suggest a simple evolutionary path from ancestral land plants to extant vascular plants. It seems likely that the appearance of vascular plants exerted selective evolutionary pressure for a more polar hormone, which would facilitate its movement through the vasculature (see Methods section for partition coefficients of these molecules). The detection of trace amounts of the JA-Ile precursor JA and its lack of activity indicate that JA had not yet been co-opted for synthesis of a functional hormone in liverworts, and in the ancestral land plant JA might have been a catabolic product of dn-OPDA. Appearance of the new hormone JA-Ile only required adaptation of two enzyme activities (OPR3 and JAR1) from pre-existing functions. OPR3 facilitated OPDA and dn-OPDA entry into the peroxisomal β-oxidation pathway, which enhanced JA production, and might have evolved from existing cytoplasmic OPR genes (**Supplementary Fig. 1**)[17,46]. The fact that JA is much more polar than dn-OPDA (see Methods) provided a selective advantage due to its systemic distribution via the vasculature[47,48]. In a more critical event, since JA is smaller than dn-OPDA, JAR1-mediated conjugation of JA to Ile provided the specificity necessary for its interaction with COI1. JAR1 belongs to the family of GH3 enzymes, which have poor substrate specificity and are involved mainly in auxin conjugation to amino acids[49]. JA-Ile is slightly larger than the "ancestral" dn-OPDA, but change of a single amino acid in the ancestral COI1 receptor easily accommodated the hormone variant. In summary, three changes (mutation of one amino acid in COI1 and modification of two pre-existing enzymes) were sufficient for the evolution of a new hormone and adaptation of its signalling pathway in vascular plants.

Co-evolution of hormone metabolites and receptor specificities are reported to broaden regulatory capabilities[50]. Although dn-*iso*-OPDA was not detected in Arabidopsis, dn-*cis*-OPDA accumulates and is currently considered simply a precursor of the vascular plant hormone JA-Ile. Our results suggest an additional hormonal role for dn-*cis*-OPDA in vascular plants, the importance of which awaits further study.

Acknowledgements We thank J. Paz-Ares and members of Solano's lab for critical reading of the manuscript and C. Mark for English editing. We thank K. Inoue (Kyoto University) for vector construction and assistance with CRISPR/Cas9^{D10A} cloning. We also thank H. Matsuura (Hokkaido Univ.) for assistance with OPDA synthesis. J. Langdale (Oxford University) kindly provided *Anthoceros agrestis* and B. Benito (CBGP-UPM-INIA) *Physcomitrella patens*. E.E. Farmer (University of Lausanne) kindly provided Methyl-dn-OPDA and M. Alfonso (EEAD-CSIC) provided dn-OPDA. L. Colombo (University of Milan) kindly provided pTFT vector. This work was funded by the Spanish Ministry for Science and Innovation grant BIO2016-77216-R (MINECO/FEDER). I.M. was supported by a predoctoral fellowship from the Ministerio de Educación, Spain (grant AP2010-1410) and EMBO Short Term Fellowship (ASTF 385-2013). This work was partly supported by MEXT KAKENHI Grant Numbers JP15K21758 and JP25113009 to TK. P.R and C. G.-D. are funded by the Swiss National Science Foundation Grant Nr. 31003A_169278

Author Contributions I.M. and R.S. designed the experiments. I.M. performed experiments in Fig. 1, 2, 4 and 6, Supplementary Fig. 1, 2, 3a, 4, 5, 6, 7 and 9, and prepared the samples for experiments in Fig. 3 and 5, and Supplementary Fig. 8. S.I. identified Mp*coi1-1*. A.M.Z quantified oxylipins (Fig. 1 and 5, and Supplementary Fig. 1 and 8). M.H. synthesized all

chemicals described in methods. J.M.F. designed and analyzed microarray data. G.G.-C. performed gene expression analysis. C.G-D. performed insect feeding assays. P.R. designed, supervised and analyzed insect feeding assays. K.T. synthesized OPDA and OPDA-Ile. J.M.G-M. designed and supervised LC-MS experiments. R.N. and T.K. designed and supervised homologous recombination and CRISPR experiments to obtain Mp*coi1* mutants. R.S. supervised the work. I.M and R.S wrote the manuscript. All authors discussed the results and edited the manuscript.

Competing financial interests

The authors declare no competing financial interests.

References

1. Howe, G. A. & Jander, G. Plant Immunity to Insect Herbivores. *Annu. Rev. Plant Biol.* **59,** 41–66 (2008).
2. Wasternack, C. & Hause, B. Jasmonates: Biosynthesis, perception, signal transduction and action in plant stress response, growth and development. An update to the 2007 review in Annals of Botany. *Annals of Botany* **111,** 1021–1058 (2013).
3. Chini, A., Gimenez-Ibanez, S., Goossens, A. & Solano, R. Redundancy and specificity in jasmonate signalling. *Current Opinion in Plant Biology* **33,** 147–156 (2016).
4. Staswick, P. E. & Tiryaki, I. The oxylipin signal jasmonic acid is activated by an enzyme that conjugates it to isoleucine in Arabidopsis. *Plant Cell* **16,** 2117–27 (2004).
5. Fonseca, S. *et al.* (+)-7-iso-Jasmonoyl-L-isoleucine is the endogenous bioactive jasmonate. *Nat. Chem. Biol.* **5,** 344–350 (2009).

6. Wasternack, C. How Jasmonates Earned their Laurels: Past and Present. *J. Plant Growth Regul.* **34,** 761–794 (2015).

7. Pratiwi, P. *et al.* Identification of Jasmonic Acid and Jasmonoyl-Isoleucine, and Characterization of AOS, AOC, OPR and JAR1 in the Model Lycophyte Selaginella moellendorffii. *Plant Cell Physiol.* **58,** 789–801 (2017).

8. Xie, D. X., Feys, B. F., James, S., Nieto-Rostro, M. & Turner, J. G. COI1: an Arabidopsis gene required for jasmonate-regulated defense and fertility. *Science* **280,** 1091–4 (1998).

9. Chini, A. *et al.* The JAZ family of repressors is the missing link in jasmonate signalling. *Nature* **448,** 666–671 (2007).

10. Thines, B. *et al.* JAZ repressor proteins are targets of the SCFCOI1 complex during jasmonate signalling. *Nature* **448,** 661–665 (2007).

11. Sheard, L. B. *et al.* Jasmonate perception by inositol-phosphate-potentiated COI1–JAZ co-receptor. *Nature* **468,** 400–405 (2010).

12. Yan, J. *et al.* The Arabidopsis CORONATINE INSENSITIVE1 Protein Is a Jasmonate Receptor. *Plant Cell* **21,** 2220–2236 (2009).

13. Pauwels, L. *et al.* NINJA connects the co-repressor TOPLESS to jasmonate signalling. *Nature* **464,** 788–91 (2010).

14. Zhang, F. *et al.* Structural basis of JAZ repression of MYC transcription factors in jasmonate signalling. *Nature* **525,** 269–273 (2015).

15. Rensing, S. A. *et al.* The Physcomitrella Genome Reveals Evolutionary Insights into the Conquest of Land by Plants. *Science* **319,** 64–69 (2008).

16. Matasci, N. *et al.* Data access for the 1,000 Plants (1KP) project. *Gigascience* **3,** 17 (2014).

17. Han, G. Evolution of jasmonate biosynthesis and signaling mechanisms. *J. Exp. Bot.*

68, 1323–1331 (2017).

18. Bowman, J. L. *et al.* Insights into Land Plant Evolution Garnered from the Marchantia polymorpha Genome. *Cell* **171,** 287–304.e15 (2017).

19. Záveská Drábková, L., Dobrev, P. I. & Motyka, V. Phytohormone Profiling across the Bryophytes. *PLoS One* **10,** e0125411 (2015).

20. Oliver, J. P. *et al.* Pythium infection activates conserved plant defense responses in mosses. *Planta* **230,** 569–579 (2009).

21. Ponce de León, I., Hamberg, M. & Castresana, C. Oxylipins in moss development and defense. *Front. Plant Sci.* **6,** 483 (2015).

22. Ludwig-Müller, J., Jülke, S., Bierfreund, N. M., Decker, E. L. & Reski, R. Moss (Physcomitrella patens) GH3 proteins act in auxin homeostasis. *New Phytol.* **181,** 323–38 (2009).

23. Stumpe, M. *et al.* The moss Physcomitrella patens contains cyclopentenones but no jasmonates: mutations in allene oxide cyclase lead to reduced fertility and altered sporophyte morphology. *New Phytol.* **188,** 740–749 (2010).

24. Yamamoto, Y. *et al.* Functional analysis of allene oxide cyclase, MpAOC, in the liverwort Marchantia polymorpha. *Phytochemistry* **116,** 48–56 (2015).

25. Koeduka, T. *et al.* Biochemical characterization of allene oxide synthases from the liverwort Marchantia polymorpha and green microalgae Klebsormidium flaccidum provides insight into the evolutionary divergence of the plant CYP74 family. *Planta* **242,** 1175–1186 (2015).

26. Wickett, N. J. *et al.* Phylotranscriptomic analysis of the origin and early diversification of land plants. *Proc. Natl. Acad. Sci. U. S. A.* **111,** E4859–E4868 (2014).

27. Koo, A. J. K., Gao, X., Daniel Jones, A. & Howe, G. A. A rapid wound signal activates the systemic synthesis of bioactive jasmonates in Arabidopsis. *Plant J.* **59,**

974–986 (2009).

28. Yan, Y. *et al.* A Downstream Mediator in the Growth Repression Limb of the Jasmonate Pathway. *Plant Cell* **19,** 2470–2483 (2007).

29. Ishizaki, K., Johzuka-Hisatomi, Y., Ishida, S., Iida, S. & Kohchi, T. Homologous recombination-mediated gene targeting in the liverwort Marchantia polymorpha L. *Sci. Rep.* **3,** 1532 (2013).

30. Ishizaki, K., Chiyoda, S., Yamato, K. T. & Kohchi, T. Agrobacterium-mediated transformation of the haploid liverwort Marchantia polymorpha L., an emerging model for plant biology. *Plant Cell Physiol.* **49,** 1084–1091 (2008).

31. Ran, F. A. *et al.* Double nicking by RNA-guided CRISPR Cas9 for enhanced genome editing specificity. *Cell* **154,** 1380–9 (2013).

32. Shen, B. *et al.* Efficient genome modification by CRISPR-Cas9 nickase with minimal off-target effects. *Nat. Methods* **11,** 399–402 (2014).

33. Kubota, A., Ishizaki, K., Hosaka, M. & Kohchi, T. Efficient Agrobacterium -Mediated Transformation of the Liverwort Marchantia polymorpha Using Regenerating Thalli. *Biosci. Biotechnol. Biochem.* **77,** 167–172 (2013).

34. Sakuma, T., Nishikawa, A., Kume, S., Chayama, K. & Yamamoto, T. Multiplex genome engineering in human cells using all-in-one CRISPR/Cas9 vector system. *Sci. Rep.* **4,** 5400 (2014).

35. Park, J.-H. *et al.* A knock-out mutation in allene oxide synthase results in male sterility and defective wound signal transduction in Arabidopsis due to a block in jasmonic acid biosynthesis. *Plant J.* **31,** 1–12 (2002).

36. Feys, B., Benedetti, C. E., Penfold, C. N. & Turner, J. G. Arabidopsis Mutants Selected for Resistance to the Phytotoxin Coronatine Are Male Sterile, Insensitive to Methyl Jasmonate, and Resistant to a Bacterial Pathogen. *Plant Cell* **6,** 751–759

(1994).

37. Katsir, L., Schilmiller, A. L., Staswick, P. E., He, S. Y. & Howe, G. A. COI1 is a critical component of a receptor for jasmonate and the bacterial virulence factor coronatine. *Proc. Natl. Acad. Sci. U. S. A.* **105,** 7100–7105 (2008).

38. Hong, F. *et al.* RankProd: a bioconductor package for detecting differentially expressed genes in meta-analysis. *Bioinformatics* **22,** 2825–7 (2006).

39. Stintzi, A., Weber, H., Reymond, P., Browse, J. & Farmer, E. E. Plant defense in the absence of jasmonic acid: The role of cyclopentenones. *Proc. Natl. Acad. Sci. U. S. A.* **98,** 12837–12842 (2001).

40. Godoy, M. *et al.* Improved protein-binding microarrays for the identification of DNA-binding specificities of transcription factors. *Plant J.* **66,** 700–711 (2011).

41. Zhang, L. *et al.* Host target modification as a strategy to counter pathogen hijacking of the jasmonate hormone receptor. *Proc. Natl. Acad. Sci. U. S. A.* **112,** 14354–14359 (2015).

42. Weber, H., Vick, B. A. & Farmer, E. E. Dinor-oxo-phytodienoic acid: a new hexadecanoid signal in the jasmonate family. *Proc. Natl. Acad. Sci. U. S. A.* **94,** 10473–8 (1997).

43. Kajikawa, M. *et al.* MpFAE3, a beta-ketoacyl-CoA synthase gene in the liverwort Marchantia polymorpha L., is preferentially involved in elongation of palmitic acid to stearic acid. *Biosci. Biotechnol. Biochem.* **67,** 1667–74 (2003).

44. Chini, A. *et al.* An OPR3-independent pathway uses 4,5-didehydrojasmonate for jasmonate synthesis. *Nat. Chem. Biol.* (2018). doi:10.1038/nchembio.2540

45. Li, H. *et al.* Efficient ASK-assisted system for expression and purification of plant F-box proteins. *Plant J.* **92,** 736–743 (2017).

46. Li, W. *et al.* Phylogenetic analysis, structural evolution and functional divergence of

the 12-oxo-phytodienoate acid reductase gene family in plants. *BMC Evol. Biol.* **9,** 90 (2009).

47. Li, Q. *et al.* Transporter-Mediated Nuclear Entry of Jasmonoyl-Isoleucine Is Essential for Jasmonate Signaling. *Mol. Plant* **10,** 695–708 (2017).

48. Bozorov, T. A., Dinh, S. T. & Baldwin, I. T. JA but not JA-Ile is the cell-nonautonomous signal activating JA mediated systemic defenses to herbivory in Nicotiana attenuata. *J. Integr. Plant Biol.* **59,** 552–571 (2017).

49. Staswick, P. E. *et al.* Characterization of an Arabidopsis enzyme family that conjugates amino acids to indole-3-acetic acid. *Plant Cell* **17,** 616–27 (2005).

50. Weng, J.-K., Ye, M., Li, B. & Noel, J. P. Co-evolution of Hormone Metabolism and Signaling Networks Expands Plant Adaptive Plasticity. *Cell* **166,** 881–893 (2016).

Figure legends

Figure 1. MpCOI1 regulates responses to OPDA. (**a**) Growth inhibitory effect of OPDA (50 µM) on 14-day-old *Marchantia polymorpha* gemmalings of WT plants (Tak-1, male, and Tak-2, female) or Mp*coi1-1*, Mp*coi1-2* and Mp*coi1-3* mutants. Experiment repeated 3 times with similar results, (n=10 plants). Scale bar, 1 cm. (**b**) Growth quantification of plants (n=5 plants) shown in **a**. (**c**) MpCOI1 complements the Mp*coi1-1* mutant. Effect of OPDA (50 µM) on WT Tak-2, Mp*coi1-1*, Mp*coi1-2* and 35S:Mp*COI1*/Mp*coi1-1* gemmalings grown for 14 days. Experiment repeated 3 times with similar results, (n=10 plants). Scale bar 1 cm. (**d**) Growth quantification of plants (n=5 plants) shown in **c**. (**e**) OPDA accumulation in Tak-1 and Mp*coi1-1* male plants (Mp*coi1-1* female backcrossed once with Tak-1). Experiment repeated twice with similar results, (n=4 independent biological samples (pools) of 11 plants each). (**f**) *Spodoptera littoralis* larval weight after 10 days feeding on *M. polymorpha* thalli of Tak-1, Tak-2, Mp*coi1-1* and complemented Mp*coi1-1*. Experiment repeated 5 times with similar results, (n=28 larvae). **b**, **d**, **e** and **f**, center lines are medians, boxes show the upper and lower quartiles and whiskers show the full data range except the outliers. Dots are individual data points in **b**, **d** and **e**. Dots in **f** are outliers. All p-values were calculated with two-tailed Student's t-test.

Figure 2. At*COI1* complements the Mp*coi1-1* mutant and confers JA-Ile/COR responsiveness to *M. polymorpha*. (**a**) Growth inhibitory effect of OPDA (50 µM), JA-Ile (50 µM) or COR (0.5 µM) on 15-day-old *M. polymorpha* gemmalings of WT Tak-2, Mp*coi1-1* mutant and the $_{pro}$Mp*EF1*:At*COI1*/Mp*coi1-1* and 35S:At*COI1*/Mp*coi1-1* complemented lines. Experiment repeated 5 times with similar results, (n=8 plants). Scale bar, 1 cm. (**b**) Growth quantification of plants (n=5 plants) shown in **a**. Center lines are medians, boxes

show the upper and lower quartiles and whiskers show the full data range except the outliers. Dots are individual data points. p-values were calculated with two-tailed Student's t-test.

Figure 3. AtCOI1 complements Mp*coi1* insensitivity to OPDA-induced gene expression. (**a**) Overlapping sets of genes upregulated (Log-ratio >1; FDR <0.05) by 2h treatment of OPDA (Up OPDA) or 2h post-wounding (Up wound) and genes downregulated (Log-ratio <-1; FDR <0.05) in two independent Mp*coi1-1* and Mp*coi1-2* alleles after 2h OPDA treatment (Down Mp*coi1*). Differentially expressed genes were evaluated by the non-parametric algorithm 'Rank Products'[38] (**b**) Clustering analysis of genes upregulated (Tak-2 OPDA 2h vs Mock) and/or downregulated by OPDA (2h) in the two Mp*coi1* alleles compared to WT (Mp*coi1-1* OPDA vs Tak-2 OPDA and Mp*coi1-2* OPDA vs Tak-1 OPDA). Clustering includes Log-ratio values of selected genes in three additional experiments: Mp*coi1-1* mutant complemented with At*COI1* in response to 2h COR treatment (At*COI1*/Mp*coi1-1* COR vs Mp*coi1-1*), Mp*coi1-2* response to 2h OPDA treatment (Mp*coi1-2* OPDA vs Mock), and Tak-2 response to wounding (2h; Wound vs Mock). Analysis was set to three clusters, in which clusters 1 (top) and 2 (centre) correspond to genes upregulated in response to OPDA and/or wounding and downregulated in both Mp*coi1* alleles, and cluster 3 (bottom), to OPDA-induced, Mp*COI1*-independent genes. Total number of genes = 282. **a** and **b**, n=3 independent biological replicates formed by 8 plants each.

Figure 4. A single amino acid of COI1 determines ligand specificity. (**a**) Growth inhibitory effect of OPDA or JA-Ile (both 50 µM) on 12-day-old *M. polymorpha* gemmalings of WT Tak-1 and Tak-2, the Mp*coi1-1* mutant, the complemented line $_{pro}$Mp*EF1*:At*COI1*/Mp*coi1-1* and the chimaeras $_{pro}$Mp*EF1*:At*COI1*$^{1-188}$-Mp*COI1*$^{188-581}$-flag/Mp*coi1-1* and $_{pro}$Mp*EF1*:Mp*COI1*$^{1-187}$-At*COI1*$^{189-592}$-flag/Mp*coi1-1*. Experiment repeated 3 times with similar results, (n=9 plants). Scale bar, 1 cm. (**b**) Growth quantification of plants shown in **a**. (**c**) Multiple sequence alignment (MSA) of amino acid sequences surrounding AtCOI1 Ala^{384} from various land plants (Mp, *Marchantia polymorpha*; Pp, *Physcomitrella patens*; Sm, *Selaginella moellendorfii*; AmTr; *Amborella trichopoda*; Os, *Oryza sativa*; Bradi; *Brachypodium distachyon*; Sl, *Solanum lycopersicum*; Nt, *Nicotiana tabacum*; At, *Arabidopsis thaliana*), showing the conservation of Ala^{384} in COI1 from all vascular plants, but not in bryophytes. The AtTIR1 sequence was included as an outgroup. MSA was performed using MUSCLE. (**d**) The V377A mutation in MpCOI1 confers responsiveness to JA-Ile and COR. Effect of OPDA, JA-Ile and COR on 13-day-old *M. polymorpha* gemmalings of WT Tak-1 and two lines of $_{pro}$Mp*EF1*:Mp*COI1*^{V377A}-flag/Mp*coi1-1*. Experiment repeated 3 times with similar results, (n=5 plants). Scale bar, 1 cm. (**e**) Growth quantification of plants shown in **d** (n=4 plants). **b** and **e**, center lines are medians, boxes show the upper and lower quartiles and whiskers show the full data range except the outliers. Dots are individual data points. p-values were calculated with two-tailed Student's t-test.

Figure 5. OPDA is a precursor of dinor-OPDA and both accumulate after wounding. (**a**) Time-course accumulation of OPDA, dinor-OPDA and dinor-*iso*-OPDA in WT Tak-1 in basal conditions or 5 min, 30 min and 2 h after mechanical wounding. Experiment repeated twice with similar results. p-values were calculated with two-tailed Student's t-test. (**b**) Accumulation of deuterated d5-dn-OPDA, d5-dn-*iso*-OPDA and d5-OPC-6 in *M. polymorpha* WT Tak-1 plants 0, 5 and 30 min after d5-OPDA treatment. **a** and **b**, n=4 independent biological samples formed by 11 plants each. Center lines are medians, boxes show the upper and lower quartiles and whiskers show the full data range. Dots are individual data points.

Figure 6. Dinor-OPDA is the bioactive ligand of MpCOI1 in *M. polymorpha*. (**a**) Structures of dinor-OPDA isomers. (**b**) Effect of various concentrations (1, 3 and 15 µM) of OPDA and dinor-OPDA isomers on gemmalings of WT Tak-2, Mp*coi1-1* and $_{pro}$Mp*EF*:At*COI1*/Mp*coi1-1*. Experiment repeated 3 times with similar results, (n=7 plants). Scale bar, 1 cm. (**c**) Growth percentage of plant area of Tak-2 by OPDA or dinor-OPDA isomers concentrations as in **b** (n=6 plants). Center lines are medians, boxes show the upper and lower quartiles and whiskers show the full data range except the outliers. Dots are individual data points. Statistical analysis by ANOVA. Letters indicate statistically significant groups. (**d**) Immunoblot (anti-flag antibody) of recovered MpCOI1-flag (from 35S:Mp*COI1*-flag Arabidopsis extracts) after pull-down reactions using recombinant MpJAZ-MBP protein alone (mock) or with indicated dinor-OPDA isomers concentrations. Bottom, Coomassie blue staining of MpJAZ-MBP after cleavage with Factor Xa. This experiment was repeated 5 times with similar results. (**e**) Dn-OPDA isomers induce MpCOI1/MpJAZ interaction in yeast. Yeast two-hybrid interaction assays between MpCOI1 and MpJAZ in the absence or presence of JA-Ile, dn-*iso*-OPDA or dn-*cis*-OPDA (all 50 µM). MpASK1 was co-expressed using pTFT vector to favor MpCOI1 stability[45]. AtJAZ9/AtJAZ9 interaction was used as a positive control. L, leucine; W, tryptophan; H, histidine; A, adenine; BD, binding domain; AD, activation domain. Co-transformed yeasts were plated on media lacking the indicated amino acids to confirm the presence of the two or three plasmids (-LW or -ALW) or assess the interaction (-HALW). This experiment was repeated 3 times with similar results. (**f**) Immunoblot (anti-flag antibody) of recovered AtCOI1-flag (from 35S:At*COI1*-flag Arabidopsis extracts) after pull-down reactions using recombinant MpJAZ-MBP protein alone (mock) or with OPDA, JA-Ile, COR, dn-*cis*-OPDA or dn-*iso*-OPDA (all 50 µM except COR 0.5 µM). Bottom, Coomassie blue staining of MpJAZ-MBP after cleavage with Factor Xa. This experiment was repeated 5 times with similar results. **d** and **f**, uncropped blots are shown in **Supplementary Fig. 10a,b**.

ON-LINE METHODS

Chemical synthesis

All details of chemical synthesis can be found in Supplementary Note 1

Plant material and growth conditions.

Marchantia polymorpha accession Takaragaike-1 (Tak-1; male) and Takaragaike-2 (Tak-2; female) were the wild-types. *M. polymorpha* (gemmae or spores) and *Anthoceros agrestis* (9 mm^2 thallus fragments) were grown on half Gamborg's B5 medium containing 1% agar under continuous light (50-60 µmol m^{-2} s^{-1}) and 20°C (n=9 plants/treatment). *Physcomitrella patens* was grown on BCDAT medium under 16-h light/8-h dark cycle at 22 °C (n=16 plants/treatment). *Arabidopsis thaliana* 35S:Mp*COI1*-flag, 35S:*MpCOI1*^{V377A}-flag and 35S:At*COI1*-flag seedlings were grown on MS medium containing 0.6% agar. *A. thaliana* Col-0 WT seedlings were grown on Johnson medium containing 0.55% agar and the indicated molecules. All *A. thaliana* plants were grown under long day conditions at 22°C. Plants used for crossing were grown on soil under continuous white light supplemented with far-red to induce gametangiophores. At least 15 archegoniophores per genotype were crossed. Spores were sterilized with 0.25% sodium hypochlorite (Sigma) and 0.05% Triton X-100. For hormone treatments, 10 gemmae per genotype and treatment were used. The compounds were incorporated into the media throughout the growth period. The quantitative data were obtained by measuring the area of plants (bryophytes) or *A. thaliana* root length; "growth percentage" refers to the ratio of treated vs untreated plants. Every experiment was repeated at least 3 times with similar results. Plant pictures were taken with a NIKON D1-x digital camera. Area of plants and root length were measured with ImageJ software.

Plant transformation.

M. polymorpha was transformed following either the sporeling transformation method for F1 or BC4 sporelings[30] or the cut-thalli transformation method[33]. *A. thaliana* was transformed by floral dipping.

Gene identification and phylogenetic analyses.

Sequences were obtained from Phytozome, http://marchantia.info, or OneKP database[16]. Sequences were aligned with MUSCLE and trees were built with PhyML using 100 bootstraps.

Gene-targeting homologous recombination.

HR to obtain Mp*coi1-1* mutant was performed as previously described[29]. Two fragments of 3.5 kb were amplified from Tak-1 genomic DNA using primers listed in **Supplementary Table 1**. Both fragments were cloned into the PacI and AscI sites of pJHY-TMp1 vector using In-Fusion cloning kit (Clontech). This vector was transferred to *A. tumefaciens* GV6620 and used for F1 sporeling transformation[30]. The mutant line carrying the T-DNA insertion in the first exon was identified by PCR using primers listed in **Supplementary Table 1** and KODFx Neo Polymerase to check that the insertion disrupted the MpCOI1 locus.

CRISPR/Cas9^{D10A} nickase-mediated mutagenesis to obtain Mp*coi1-2* and Mp*coi1-3* mutants.

Four different gRNAs (**Supplementary Table 1**) were cloned into the BsaI site of pMpGE_En04 vector [vector modified from pMpGE_En03 (Addgene plasmid #71535) to insert BglI site at the EcoRI site] or into the multiplex vectors pBC-GE12, pBC-GE23 or pBC-GE34[31,32,34]. The four gRNAs cassettes were cloned then into pMpGE017 binary vector carrying the Cas9^{D10A} (nickase)[31,32,34] by LR reaction (Invitrogen). The $_{pro}$Mp*EF*:*Cas9^{D10A}* cassette was cloned into the Aor51HI-SacI site of pMpGWB101[51] to generate pMpGE017 vector. The final construct of pMpGE017 was transferred to *Agrobacterium tumefaciens* strain GV6620. *M. polymorpha* F1 spores and cut-thalli (Tak-1) were transformed and transformants selected on hygromycin, genotyped and sequenced.

Cloning and transformation.

Sequences of Mp*COI1* (Mapoly0025s0025), Mp*JAZ* (Mapoly0097s0021), Mp*ASK1* (Mapoly0007s0013), chimaeras Mp*COI1*$^{1-187}$-At*COI1*$^{189-592}$ and At*COI1*$^{1-188}$-Mp*COI1*$^{188-581}$ and the point mutation Mp*COI1*^{V377A} were amplified from Tak-1 cDNA (for WT genes) or plasmids containing At*COI1* or Mp*COI1* to introduce mutations with Expand High Fidelity (Roche) using specific primers (**Supplementary Table 1**) and cloned into pDONR207 (BP reaction; Invitrogen). The plasmid pDONR207 At*COI1* was already available[5]. LR reaction (Invitrogen) was used to clone Mp*JAZ* into pKM596 and pGADT7; Mp*COI1* into pGBKT7, pMpGWB111 and 311; Mp*ASK1* into pTFT; At*COI1* into pMpGWB310 and 311; Mp*COI1*^{V377A} into pMpGWB111 and 310; and the chimaeras into pMpGWB310[51]. BC4 sporelings were transformed with the construct pMpGWB111 Mp*COI1*[30].

Protein extraction and pull-down assays.

These assays were performed with Arabidopsis transgenic extracts as previously described[5,52]. Every assay was repeated 4-5 times with similar results.

Yeast two-hybrid assays.

This assay was performed as previously described[53]. MpASK1 was expressed in the pTFT vector (kindly provided by L. Colombo, University of Milan) to facilitate MpCOI1 protein stability[45]. AtJAZ9 dimer was used as a positive control[54]. Yeast growth 7 days after incubation at 28ºC was scored as positive interaction. This experiment was repeated 3 times with similar results.

Herbivory assays.

M. polymorpha gemmae were grown on half Gamborg's medium (Duchefa) containing 1% agar in continuous light (20°C, 120 µmol m^{-2} s^{-1}) for seven days before being transferred to soil (three per pot). Thalli were then grown for five weeks in a growth chamber (21°C, 10/14 h light/dark cycle, 100 µmol m^{-2} s^{-1}) using a lid to cover the tray and maintain high humidity. For insect assays, experiments were performed with 6-week-old *M. polymorpha* thalli in transparent plastic boxes. For each experiment, a total of 60 neonate *Spodoptera littoralis* larvae (eggs obtained from Syngenta) were placed on eighteen thalli. After 9 to 10 days of feeding, larvae were collected and weighed using a precision balance (Mettler-Toledo XP205). This experiment was repeated five times with similar results.

Gene expression analysis.

A custom Marchantia microarray was designed using Agilent's eArray tool (https://earray.chem.agilent.com/earray/). Fasta files for target transcripts (Mpolymorpha_320_v3.1.transcript_primaryTranscript.fa and Mpolymorpha_320_v3.1.transcript.fa) were obtained from Phytozome v12.0 web portal (https://phytozome.jgi.doe.gov), and contained 19,287 and 24,674 transcripts, respectively, corresponding to 19,287 loci. Two probes per primary transcript were designed, following eArray's recommendations for eukaryotic transcriptomes (60 nucleotides long, with base composition and best probe methodologies in sense orientation). This step yielded two probe groups of 19,216 probes each that passed quality filters. In a second step, we selected different splicing isoforms as target transcripts to design specific probes, applying the same parameters as above. After filtering new probes not included in previous batches, this analysis generated a third probes group with 1,990 probes. Finally, an Agilent microarray in 8x60k format was designed (ID 084032) that included two copies of one of the probe groups obtained during first step (that corresponded to the most 3'-end matching probes), and one copy of the second and third groups, making in total 60,103 probes with at least 3 probes per gene.

Marchantia RNA extraction, processing, probe preparation, hybridization and bioinformatics analyses were performed as previously described[38,55], using three independent biological replicates per treatment.

Clustering of genes was performed using K-Means with euclidean distance[56] in Multi Experiment Viewer (http://mev.tm4.org/), and Venn diagrams obtained with BioVenn[57]. Promoter regions (1 kb upstream the annotated transcription start site) were obtained using BEDTOOLS[58] from the Marchantia genome sequence (Mpolymorpha_320_v3.0.fa) and the annotation file (Mpolymorpha_320_v3.1.gene.gff3), both downloaded from Phytozome. Sequence scan for the perfect G-box (CACGTG) was performed with the 'dna-pattern' tool in RSAT[59].

Expression of Mp*COI1* and OPDA-marker genes was analysed by Q-PCR using Mp*ACT* or Mp*APT* as control (**Supplementary Table 1**). This experiment was repeated twice with similar results. Heatmap was built with Multi Experiment Viewer.

Statistical analysis.

Statistical significance based on two-tailed Student's *t*-test analysis was calculated using Excel (Microsoft). ANOVA was performed with R commander.

Hormone measurements.

Mechanical wounding was performed with tweezers all over the 21-day-old thalli of Tak-1. Alternatively, plants were transferred to a 6-well plate containing liquid 0.5 Gamborg's B5 and deuterated compounds (d5-18:3, d6-16:3 or d5-OPDA) for the indicated times. 4 independent biological replicates (11 thalli each) were measured per time point. Plants were ground in liquid nitrogen prior hormone measurements. (-)-Jasmonic acid (JA), *cis*-12-oxo-phytodienoic acid (OPDA) and N-(-)-jasmonoyl isoleucine (JA-Ile) were purchased from OlChemim Ltd (Olomouc, Czech Republic), dinor-12-oxo-phytodienoic acid (dn-OPDA) from Cayman Chemical Company (Ann Arbor, MI, USA) and 4,5-ddh-JA, 4,5-ddh-JA-Ile, OPDA-Ile[60], dn-*iso*-OPDA, tn-*iso*-OPDA, 3,7-ddh-JA and 3,7-ddh-JA-Ile-Me were synthesized (see below). OPC-6 was already available[5]. The deuterium-labeled internal standards $^{2}H_{2}$-N-(-)-jasmonoyl isoleucine (d2-JA-Ile) and $^{2}H_{5}$-*cis*-12-oxo-phytodienoic acid (d5-OPDA) were obtained from OlChemim Ltd., $^{2}H_{5}$-

jasmonic acid (d5-JA) from CDN Isotopes (Pointe-Claire, Quebec, Canada) and $^{2}H_5$-dinor-12-oxo-phytodienoic acid (d5-dnOPDA) from Cayman Chemical Co.

Endogenous JA, JA-Ile, OPDA, dn-OPDA, dn-*iso*-OPDA, OPC-6, 4,5-ddh-JA and 4,5-ddh-JA-Ile and the corresponding $^{2}H_5$-derivatives in plants were analyzed using high performance liquid chromatography-electrospray-high-resolution accurate mass spectrometry (HPLC-ESI-HRMS). The hormones were extracted and purified as follows: 0.25 g frozen plant tissue (ground to a powder in a mortar with liquid N_2) was homogenized with 2.5 ml precooled (-20ºC) methanol:water:HCOOH (90:9:1, v/v/v with 2.5 mM Na-diethyldithiocarbamate) and 25 µl of a stock solution of 1000 ng ml^{-1} deuterium-labeled internal standards d5-JA and d5-dnOPDA, 200 ng ml^{-1} d2-JA-Ile and 400 ng ml^{-1} d5-OPDA in methanol. Samples were extracted by shaking in a Multi Reax shaker (Heidolph Instruments) (60 min, 2000 rpm, room temperature). After extraction, solids were separated by centrifugation (10 min, 20,000 G, 4ºC) in a Sigma 4-16K Centrifuge, and re-extracted with 1.25 ml extraction mixture, followed by shaking (20 min) and centrifugation. Pooled supernatants (2 ml) were separated and evaporated at 40ºC in a RapidVap Evaporator (Labconco Co., Kansas City, MO). The residue was redissolved in 500 µl methanol/0.133% acetic acid (40:60, v/v) and centrifuged (10 min, 20,000 RCF, 4ºC) before injection into the HPLC-ESI-HRMS system.

Hormones were quantified using a Dionex Ultimate 3000 UHPLC device coupled to a Q Exactive Focus Mass Spectrometer (Thermo Fisher Scientific) equipped with an HESI(II) source, a quadrupole mass filter, a C-trap, a HCD collision cell and an Orbitrap mass analyzer, using a reverse-phase column (Synergi 4 mm Hydro-RP 80A, 150 x 2 mm; Phenomenex, Torrance, CA). A linear gradient of methanol (A), water (B) and 2% acetic acid in water (C) was used: 38% A for 3 min, 38% to 96% A in 12 min, 96% A for 2 min and 96% to 38% A in 1 min, followed by stabilization for 4 min. The percentage of C remained constant at 4%. Flow rate was 0.30 ml min^{-1}, injection volume 40 µl, and column and sample temperatures were 35 and 15ºC, respectively. Ionization source working parameters were optimized (see **Supplementary Table 2**).

For phytohormone detection and quantification, we used a full MS experiment with MS/MS confirmation in the negative-ion mode, using multilevel calibration curves with the internal standards. MS^1 extracted from the full MS spectrum was used for quantitative analysis, and MS^2 for confirmation of target identity. For full MS, a m/z scan range from 62 to 550 was selected, resolution set at 70,000 full width at half maximum (FWHM), automatic gain control (AGC) target at $1e^6$ and maximum injection time (IT) at 250 ms. A mass tolerance of 5 ppm was accepted. The MS/MS confirmation parameters were resolution of 17,500 FWHM, isolation window of 3.0 m/z, AGC target of $2e^5$, maximum IT of 60 ms, loop count of 1 and minimum AGC target of $3e^3$. Instrument control and data processing were carried out with TraceFinder 3.3 EFS software. Accurate masses of phytohormones and internal standard and their principal fragments are shown in **Supplementary Note Table 1**, with the exception of $^{2}H_5$-JA-Ile, $^{2}H_5$-4,5-ddh-JA, $^{2}H_5$-ddh-JA-Ile, $^{2}H_5$-OPC-4, $^{2}H_5$-OPC-6 and [$^{2}H_5$]-tn-OPDA.

As an estimation of molecule polarity we used the partition coefficient (octanol-water; XlogP3-AA) for each of the molecules: OPDA (4.7), dn-OPDA (3.6), JA (1.6), (-)-JA-Ile (2.7) and (+)-7-iso-JA-Ile (3.3). Links to these values can be found here:

https://pubchem.ncbi.nlm.nih.gov/compound/5280411#section=Computed-Properties

https://pubchem.ncbi.nlm.nih.gov/compound/91746127#section=Computed-Properties

https://pubchem.ncbi.nlm.nih.gov/compound/Jasmonic_acid#section=Computed-Properties

https://pubchem.ncbi.nlm.nih.gov/compound/5497150#section=Computed-Properties

https://pubchem.ncbi.nlm.nih.gov/compound/54758681#section=Computed-Properties

Data Availability

Microarray data are available at GEO (GSE99727)

Reprints and permissions information is available at www.nature.com/reprints

Correspondence and requests for materials should be addressed to rsolano@cnb.csic.es

Full data is available upon request to rsolano@cnb.csic.es

Methods-only references

51. Ishizaki, K. *et al.* Development of gateway binary vector series with four different selection markers for the liverwort marchantia polymorpha. *PLoS One* **10,** 1–13 (2015).

52. Fonseca, S. & Solano, R. in *Jasmonate Signaling: Methods and Protocols* (eds. Goossens, A. & Pauwels, L.) **1011,** 159–171 (Humana Press, 2013).

53. Chini, A. in *Plant Chemical Genomics: Methods and Protocols* (eds. Hicks, G. R. & Robert, S.) **1056,** 35–43 (Humana Press, 2014).

54. Chini, A., Fonseca, S., Chico, J. M., Fernández-Calvo, P. & Solano, R. The ZIM domain mediates homo- and heteromeric interactions between Arabidopsis JAZ proteins. *Plant J.* **59,** 77–87 (2009).

55. Monte, I. *et al.* Rational design of a ligand-based antagonist of jasmonate perception. *Nat. Chem. Biol.* **10,** 671–6 (2014).

56. Soukas, A., Cohen, P., Socci, N. D. & Friedman, J. M. Leptin-specific patterns of gene expression in white adipose tissue. *Genes Dev.* **14,** 963–80 (2000).

57. Hulsen, T., de Vlieg, J. & Alkema, W. BioVenn - a web application for the comparison and visualization of biological lists using area-proportional Venn diagrams. *BMC Genomics* **9,** 488 (2008).

58. Quinlan, A. R. & Hall, I. M. BEDTools: a flexible suite of utilities for comparing

genomic features. *Bioinformatics* **26,** 841–2 (2010).

59. Medina-Rivera, A. *et al.* RSAT 2015: Regulatory Sequence Analysis Tools. *Nucleic Acids Res.* **43,** W50–W56 (2015).

60. Floková, K. *et al.* A previously undescribed jasmonate compound in flowering Arabidopsis thaliana – The identification of cis-(+)-OPDA-Ile. *Phytochemistry* **122,** 230–237 (2016).

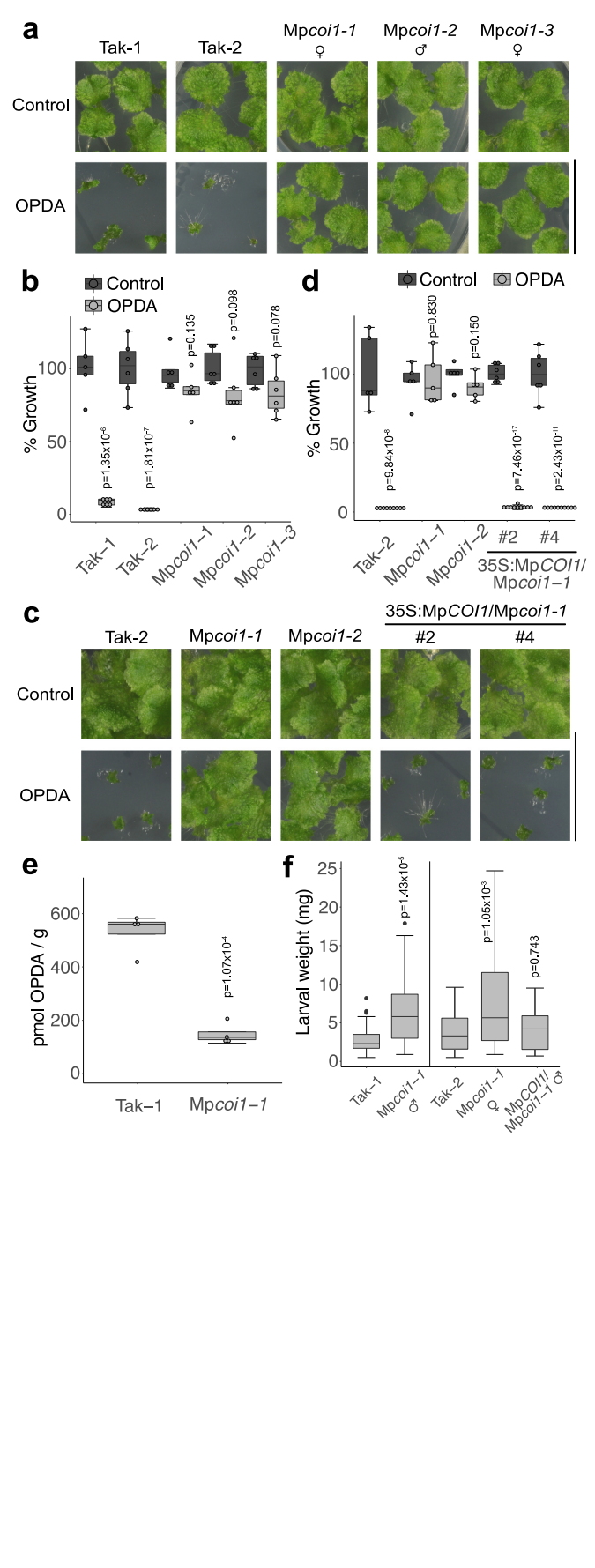
a
Tak-1
Tak-2
Mpcoi1-1 ♀
Mpcoi1-2 ♂
Mpcoi1-3 ♀
Control
OPDA
b
Control
OPDA
% Growth
100
50
0
p=1.35x10-6
p=1.81x10-7
p=0.135
p=0.098
p=0.078
Tak−1
Tak−2
Mpcoi1−1
Mpcoi1−2
Mpcoi1−3
d
Control
OPDA
% Growth
100
50
0
p=9.84x10-8
p=0.830
p=0.150
p=7.46x10-17
p=2.43x10-11
Tak−2
Mpcoi1−1
Mpcoi1−2
#2
#4
35S:MpCOI1/
Mpcoi1−1
c
35S:MpCOI1/Mpcoi1-1
Tak-2
Mpcoi1-1
Mpcoi1-2
#2
#4
Control
OPDA
e
pmol OPDA / g
600
400
200
0
p=1.07x10-4
Tak−1
Mpcoi1−1
f
Larval weight (mg)
25
20
15
10
5
0
p=1.43x10-5
p=1.05x10-3
p=0.743
Tak−1
Mpcoi1−1 ♂
Tak−2
Mpcoi1−1 ♀
MpCOI1/
Mpcoi1−1 ♂

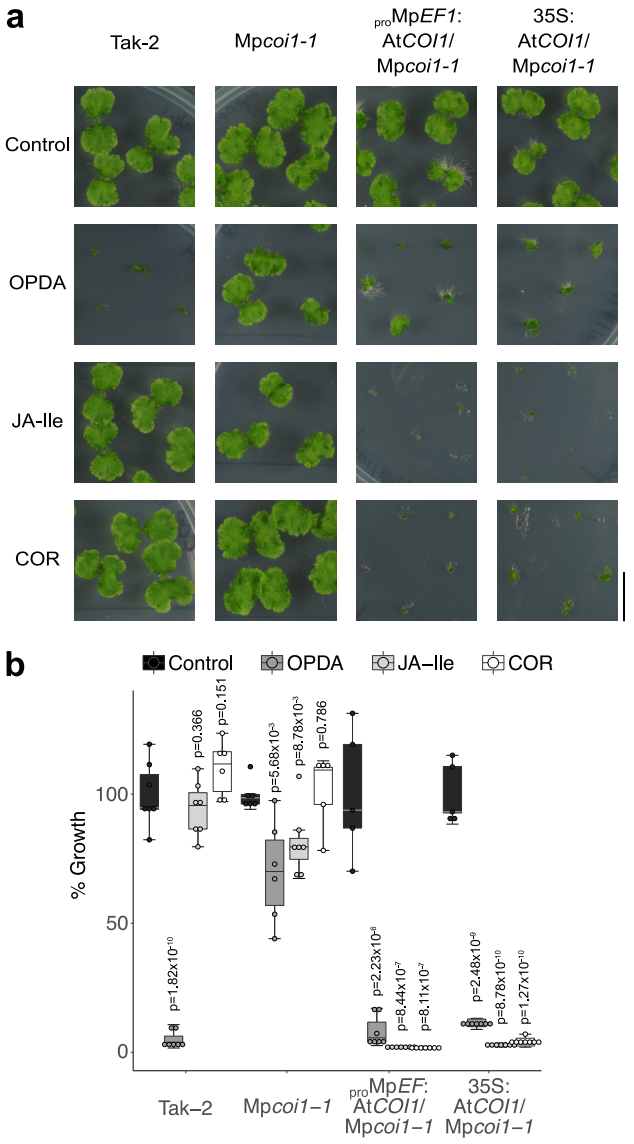
a
Tak-2
Mpcoi1-1
proMpEF1: AtCOI1/ Mpcoi1-1
35S: AtCOI1/ Mpcoi1-1
Control
OPDA
JA-Ile
COR
b
Control
OPDA
JA–Ile
COR
% Growth
100
50
0
p=1.82x10-10
p=0.366
p=0.151
p=5.68x10-3
p=8.78x10-3
p=0.786
p=2.23x10-8
p=8.44x10-7
p=8.11x10-7
p=2.48x10-9
p=8.78x10-10
p=1.27x10-10
Tak–2
Mpcoi1–1
proMpEF: AtCOI1/ Mpcoi1–1
35S: AtCOI1/ Mpcoi1–1

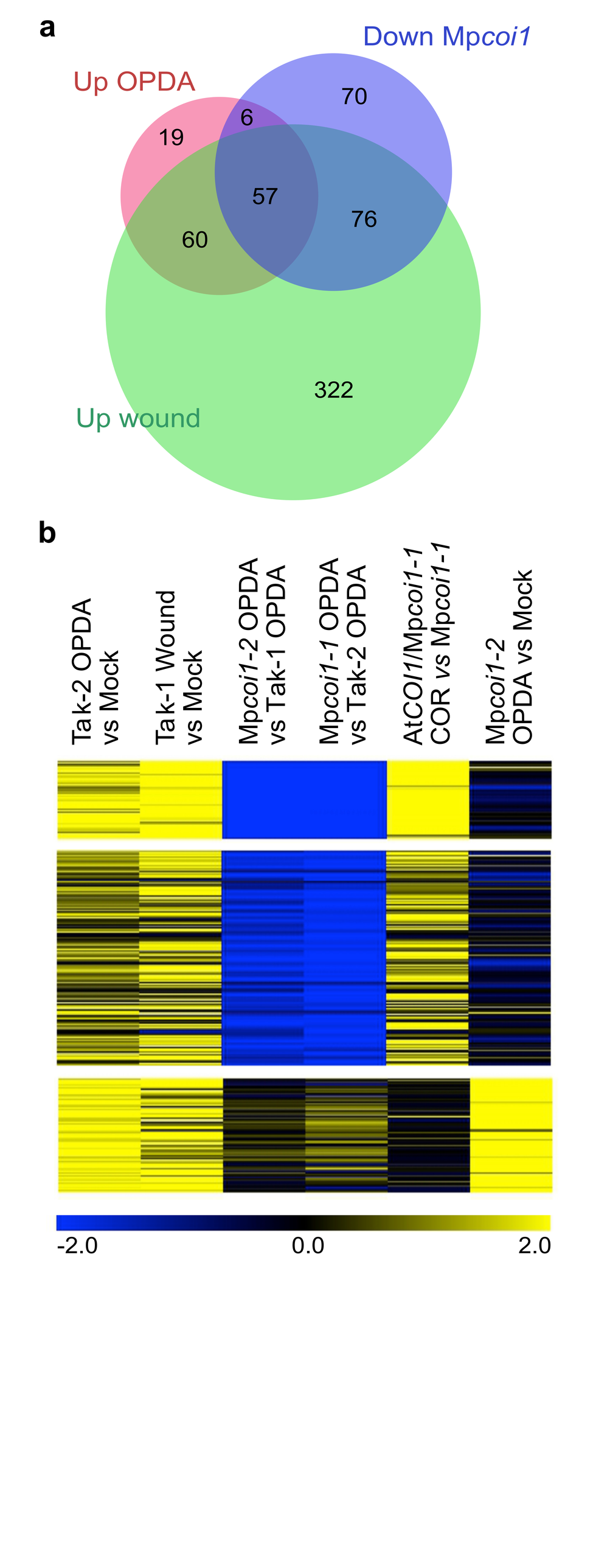
a
Down Mpcoi1
Up OPDA
70
6
19
57
76
60
322
Up wound
b
Tak-2 OPDA vs Mock
Tak-1 Wound vs Mock
Mpcoi1-2 OPDA vs Tak-1 OPDA
Mpcoi1-1 OPDA vs Tak-2 OPDA
AtCOI1/Mpcoi1-1 COR vs Mpcoi1-1
Mpcoi1-2 OPDA vs Mock
-2.0
0.0
2.0

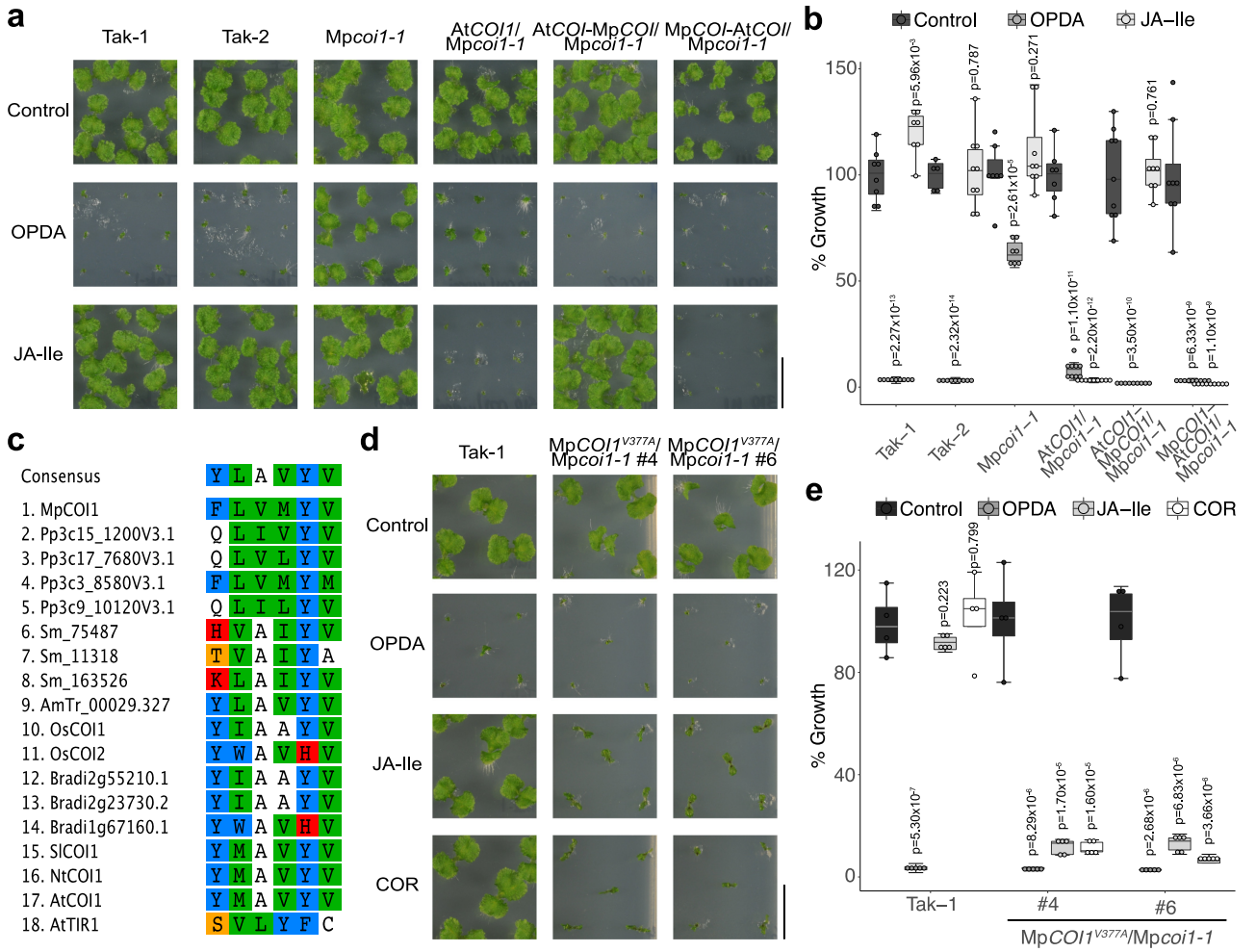
a
Tak-1
Tak-2
Mpcoi1-1
AtCOI1/ Mpcoi1-1
AtCOI-MpCOI/ Mpcoi1-1
MpCOI-AtCOI/ Mpcoi1-1
Control
OPDA
JA-Ile
b
Control
OPDA
JA–Ile
% Growth
150
100
50
0
p=2.27x10-13
p=5.96x10-3
p=2.32x10-14
p=0.787
p=2.61x10-5
p=0.271
p=1.10x10-11
p=2.20x10-12
p=3.50x10-10
p=0.761
p=6.33x10-9
p=1.10x10-9
Tak–1
Tak–2
Mpcoi1–1
AtCOI1/ Mpcoi1–1
AtCOI1– MpCOI1/ Mpcoi1–1
MpCOI1– AtCOI1/ Mpcoi1–1
c
Consensus
1. MpCOI1
2. Pp3c15_1200V3.1
3. Pp3c17_7680V3.1
4. Pp3c3_8580V3.1
5. Pp3c9_10120V3.1
6. Sm_75487
7. Sm_11318
8. Sm_163526
9. AmTr_00029.327
10. OsCOI1
11. OsCOI2
12. Bradi2g55210.1
13. Bradi2g23730.2
14. Bradi1g67160.1
15. SlCOI1
16. NtCOI1
17. AtCOI1
18. AtTIR1
d
Tak-1
MpCOI1V377A/ Mpcoi1-1 #4
MpCOI1V377A/ Mpcoi1-1 #6
Control
OPDA
JA-Ile
COR
e
Control
OPDA
JA–Ile
COR
% Growth
120
80
40
0
p=5.30x10-7
p=0.223
p=0.799
p=8.29x10-6
p=1.70x10-5
p=1.60x10-5
p=2.68x10-6
p=6.83x10-6
p=3.66x10-6
Tak–1
#4
#6
MpCOI1V377A/Mpcoi1-1

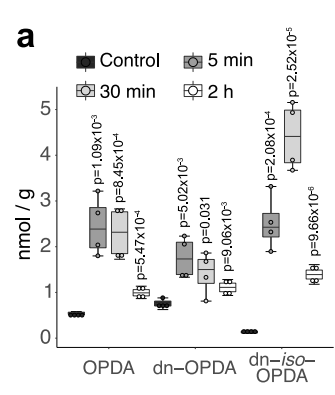
a
Control
5 min
30 min
2 h
nmol / g
0
1
2
3
4
5
p=1.09x10-3
p=8.45x10-4
p=5.47x10-4
p=5.02x10-3
p=0.031
p=9.06x10-3
p=2.08x10-4
p=2.52x10-5
p=9.66x10-6
OPDA
dn–OPDA
dn–iso–OPDA

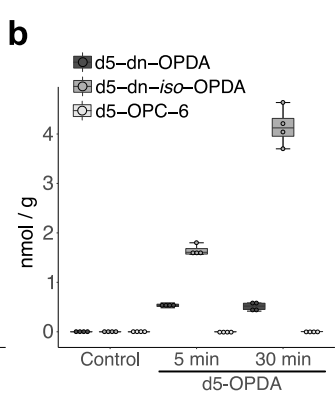
b
d5–dn–OPDA
d5–dn–iso–OPDA
d5–OPC–6
nmol / g
0
1
2
3
4
Control
5 min
30 min
d5-OPDA

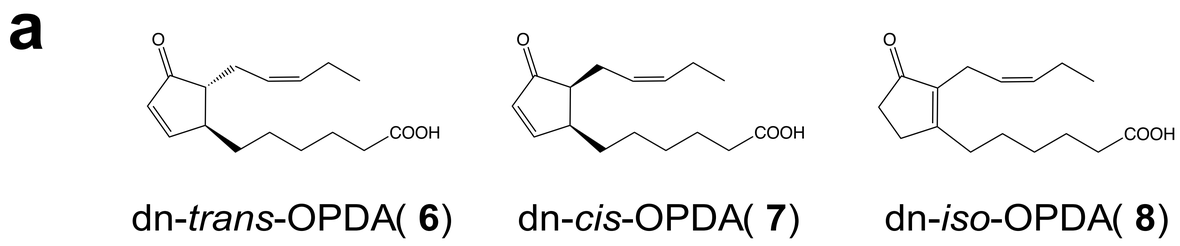
a
O
COOH
dn-*trans*-OPDA(**6**)
dn-*cis*-OPDA(**7**)
dn-*iso*-OPDA(**8**)

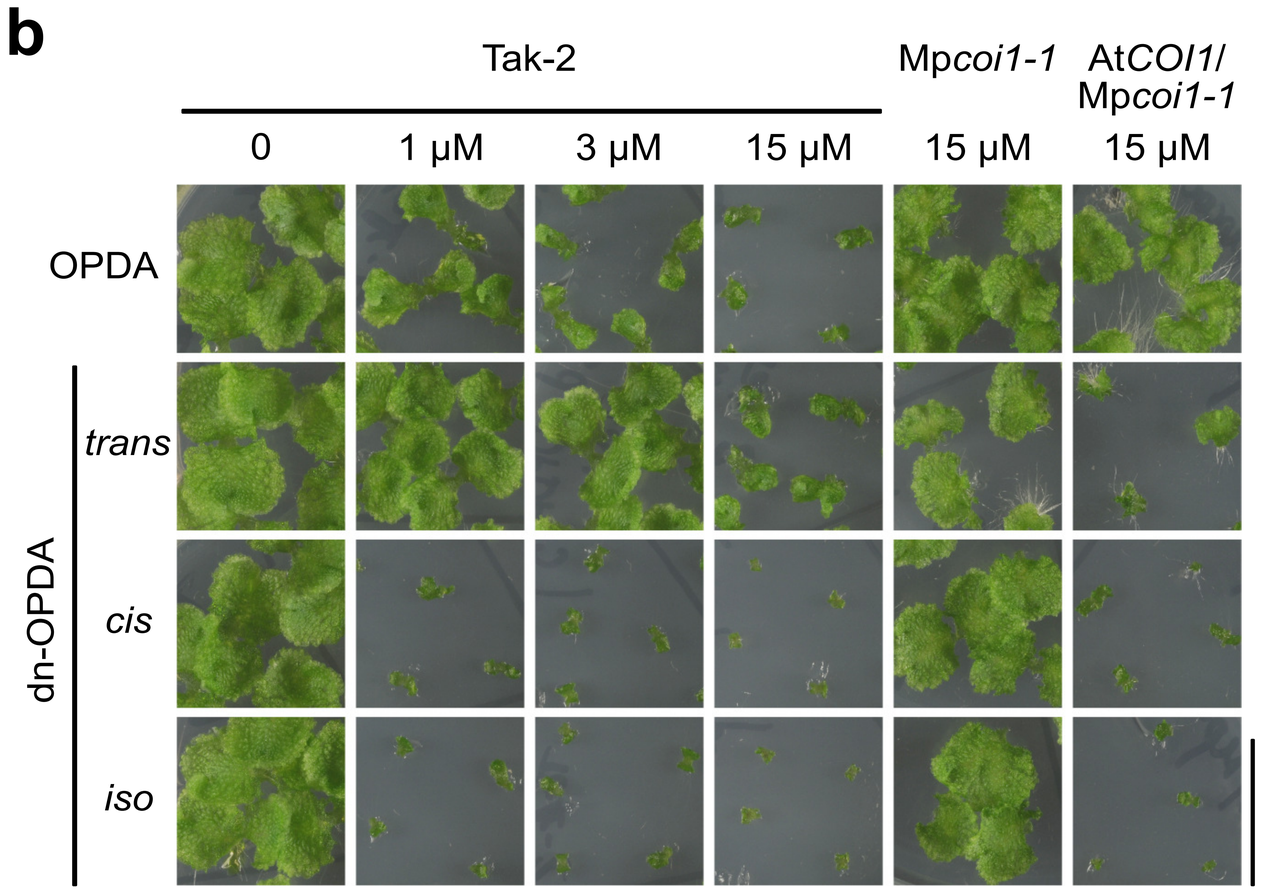
b
Tak-2
Mp*coi1-1*
At*COI1*/
Mp*coi1-1*
0
1 μM
3 μM
15 μM
15 μM
15 μM
OPDA
dn-OPDA
trans
cis
iso

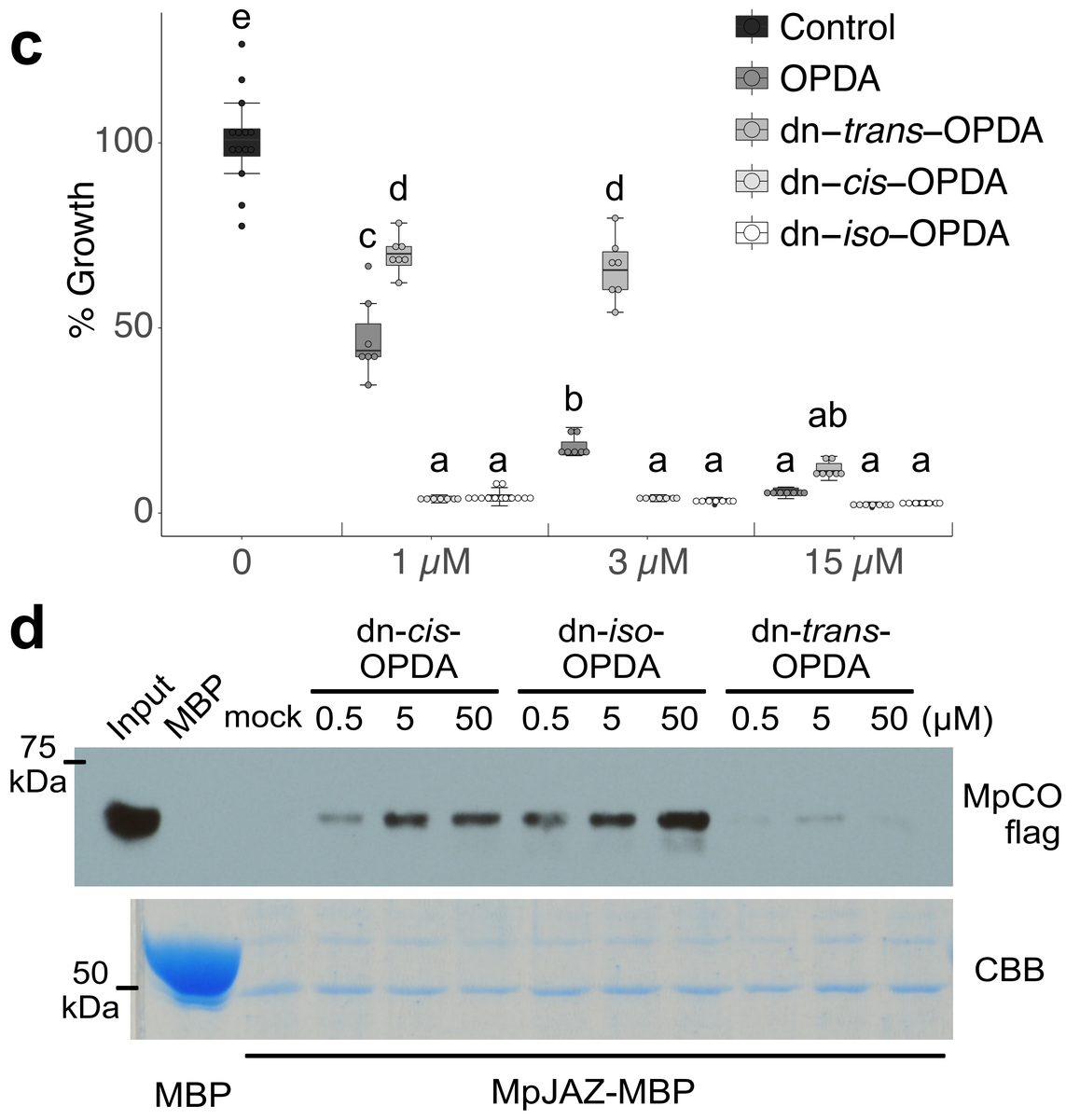
c
% Growth
100
50
0
Control
OPDA
dn–*trans*–OPDA
dn–*cis*–OPDA
dn–*iso*–OPDA
e
d
c
b
ab
a
0
1 μM
3 μM
15 μM
d
dn-*cis*-
OPDA
dn-*iso*-
OPDA
dn-*trans*-
OPDA
Input
MBP
mock
0.5
5
50
(μM)
75
kDa
MpCOI1-
flag
50
kDa
CBB
MBP
MpJAZ-MBP

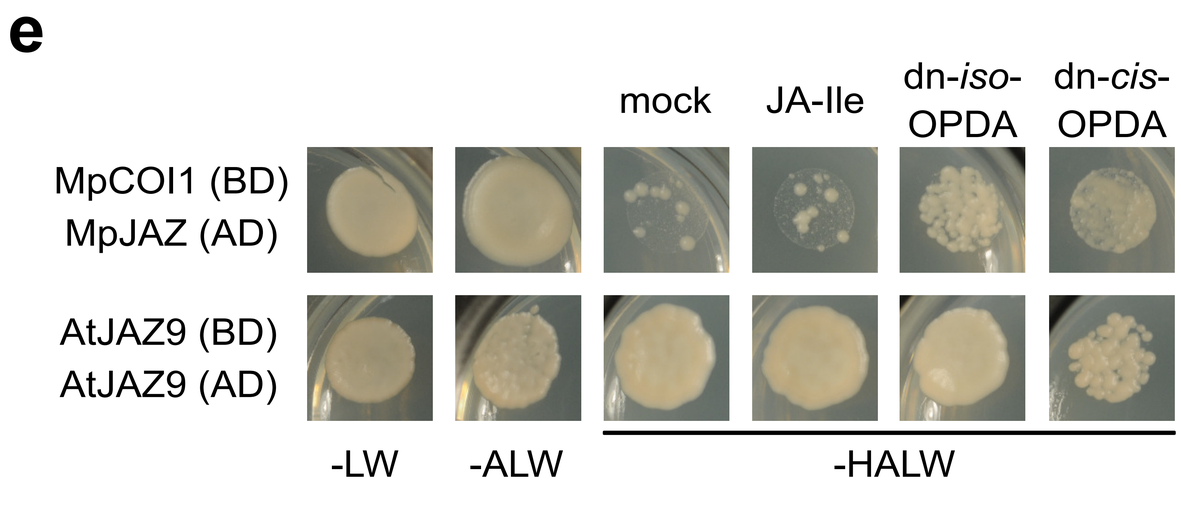
e
mock
JA-Ile
dn-*iso*-
OPDA
dn-*cis*-
OPDA
MpCOI1 (BD)
MpJAZ (AD)
AtJAZ9 (BD)
AtJAZ9 (AD)
-LW
-ALW
-HALW

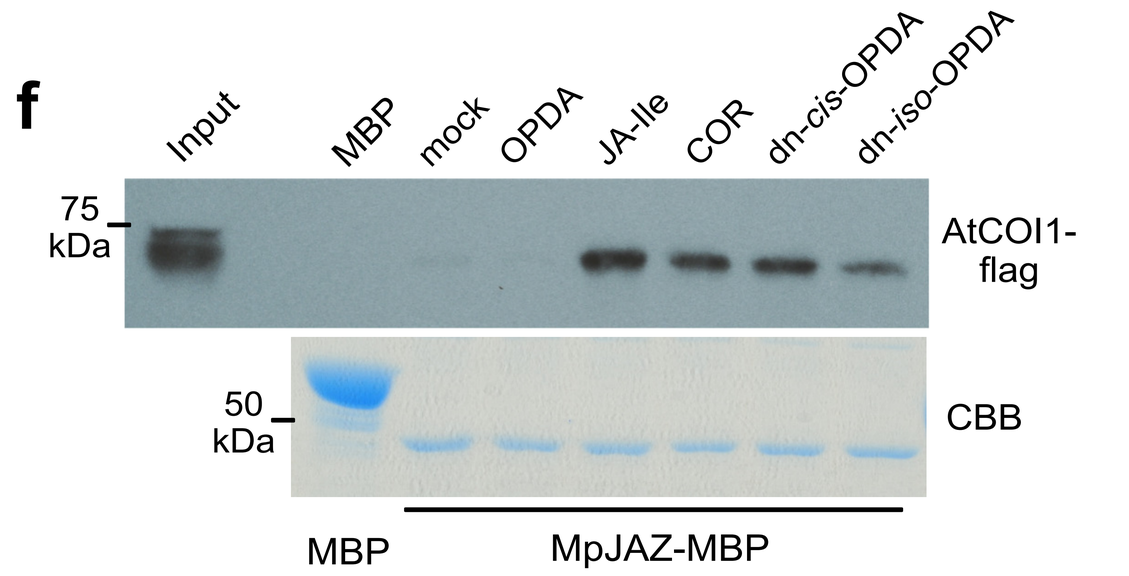
f
Input
MBP
mock
OPDA
JA-Ile
COR
dn-*cis*-OPDA
dn-*iso*-OPDA
75
kDa
AtCOI1-
flag
50
kDa
CBB
MBP
MpJAZ-MBP

Marchantia polymorpha

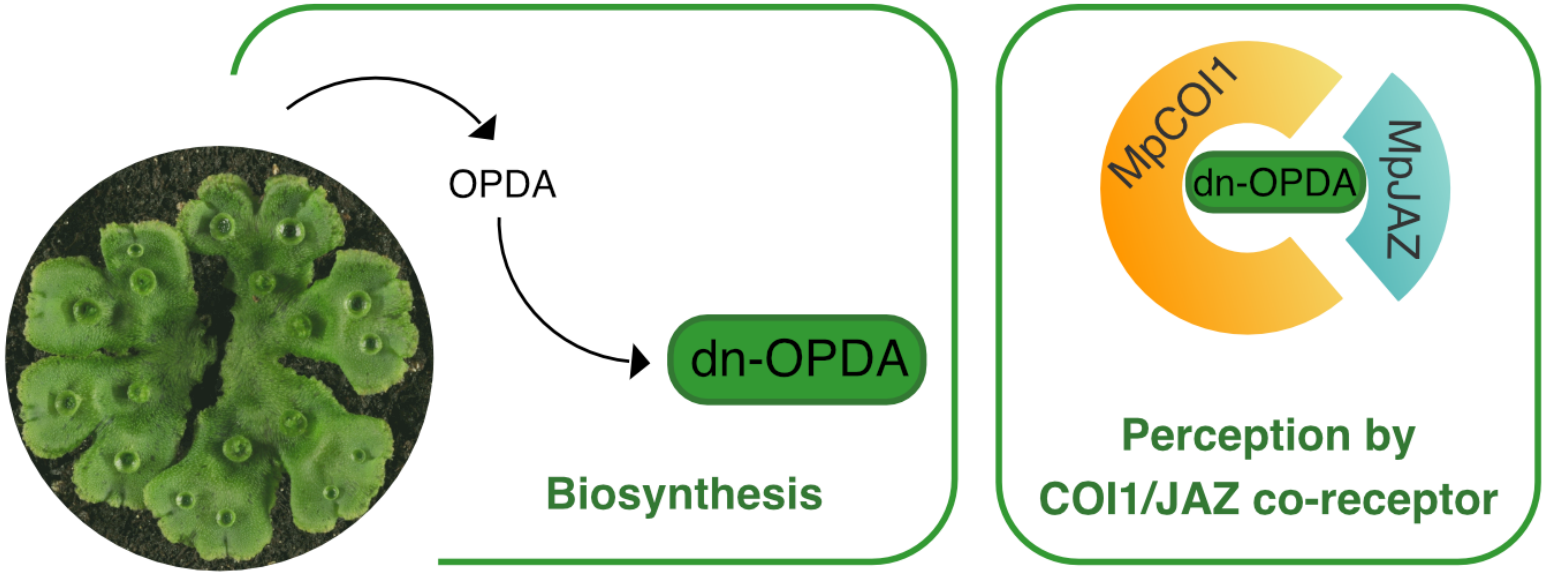

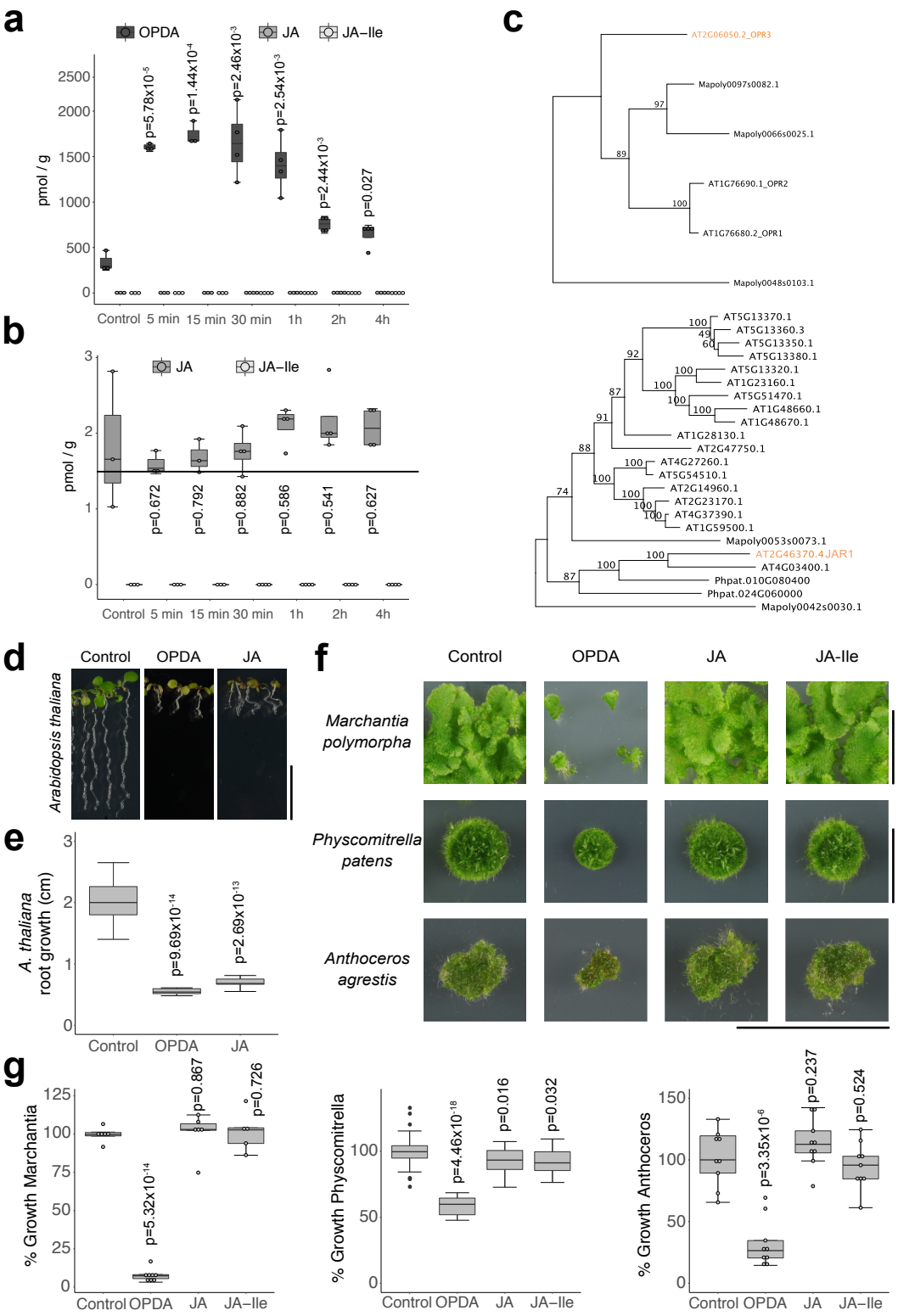

Supplementary Figure 1. OPDA accumulates after wounding and inhibits growth in bryophytes. (**a**) Time-course of OPDA, JA and JA-Ile accumulation in *Marchantia polymorpha* WT Tak-1 at different times after mechanical wounding. This experiment was repeated twice with similar results, (n=3 independent biological replicates of 11 plants each). (**b**) Magnification of a to show that JA levels detected in *M. polymorpha* were near the detection limit (black horizontal line). (**c**) Phylogenetic analyses of OPR3 (top) and JAR1 (bottom) in *M. polymorpha* and *Arabidopis thaliana*. For the JAR1 tree, *Physcomitrella patens* sequences were included as a reference of bryophyte auxin-conjugating GH3. (**d**) Growth inhibitory effect of OPDA 5 μM and JA 50 μM on 7-day-old *A. thaliana* Col-0 seedlings. This experiment was repeated 5 times with similar results, (n=12 plants). Scale bar, 1 cm. (**e**) Root growth quantification of seedlings shown in **d** (n=11 plants). (**f**) Effect of OPDA, JA and JA-Ile on *M. polymorpha* WT Tak-1 (n=8 plants), *P. patens* (n=16 plants) and *Anthoceros agrestis* (n=9 plants) growth. Concentration was 50 μM for all molecules. This experiment was repeated three times with similar results. Scale bars, 1 cm. (**g**) Growth quantification of plants shown in **f** (n=5, 14 and 9 plants, respectively). **a**, **b**, **e** and **g**, center lines are medians, boxes show the upper and lower quartiles and whiskers show the full data range except the outliers. p-values were calculated with two-tailed Student's t-test. Dots are outliers in the second graph of **g** and individual data points in the rest (**a**, **b** and **g**).

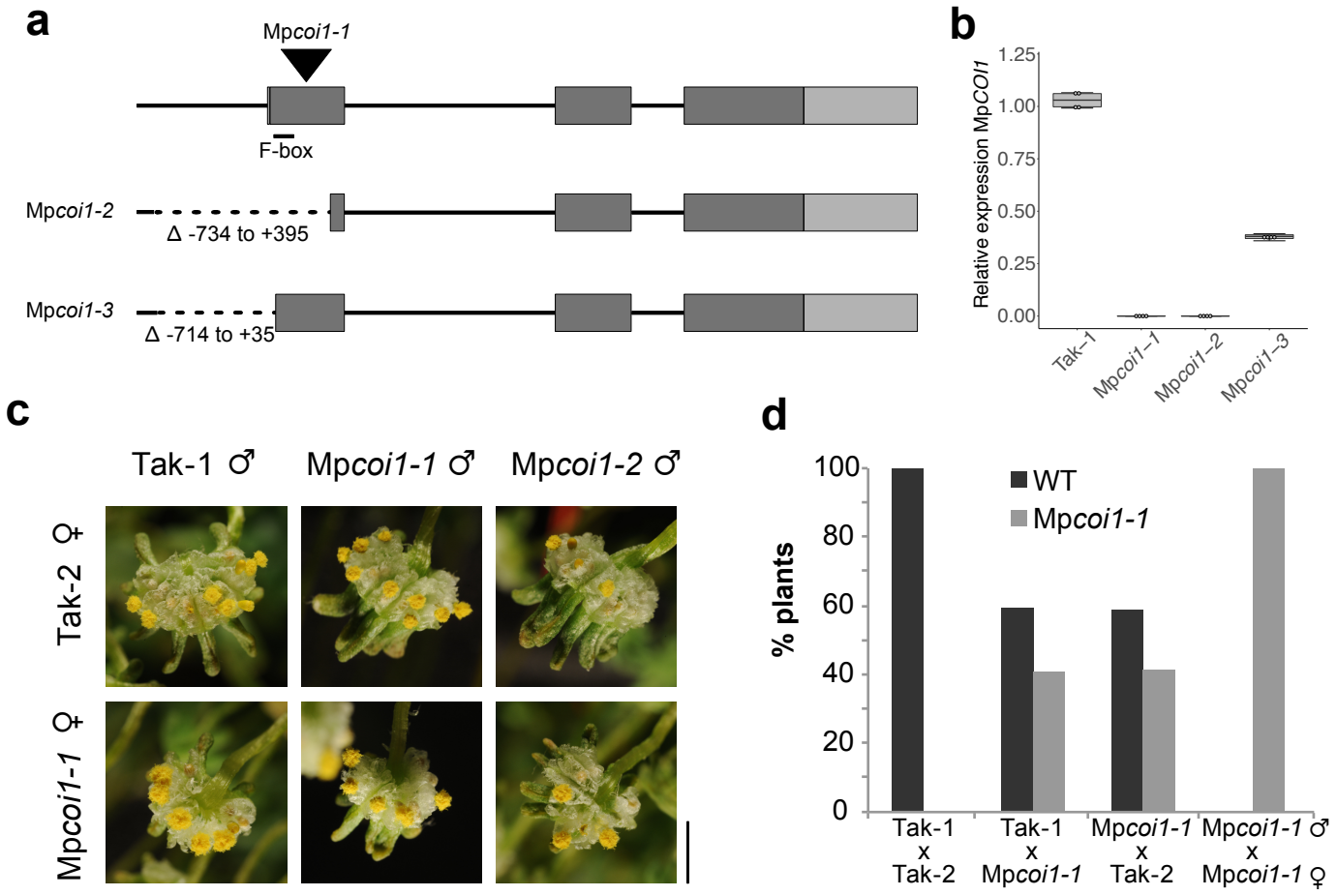

Supplementary Figure 2. Mp*coi1* mutant alleles. (**a**) Scheme of the Mapoly0025s0025 (Mp*COI1*) locus and mutant alleles. Dark grey blocks, exons; light grey, 3' UTR regions; triangle, T-DNA insertion in Mp*coi1-1* allele, which disrupts the first exon by gene targeting-mediated homologous recombination. Dashed lines indicate deletions in Mp*coi1-2* and Mp*coi1-3* mutants obtained by CRISPR/Cas9 nickase. Numbers correspond to nucleotide position of each deletion relative to ATG. In Mp*coi1-3* the first ATG is in position 355 of WT Mp*COI1* and therefore the putative truncated protein lacks the F-box domain. (**b**) Relative expression of Mp*COI1* by Q-PCR in WT Tak-1 and the three alleles Mp*coi1-1*, Mp*coi1-2* and Mp*coi1-3*. Primers amplify the 50 bp fragment from nucleotide 217 to 267 in the first exon. This experiment was repeated twice with similar results. (n=1 biological replicate formed by 6 plants). Center lines are medians, boxes show the upper and lower quartiles and whiskers show the full data range. Dots show data from 4 technical replicates. (**c**) Mature sporangia from crossing parental lines Tak-1 ♂ x Tak-2 ♀, Tak-1 ♂ x Mp*coi1-1* ♀, Mp*coi1-1* ♂ x Tak-2 ♀, Mp*coi1-1* ♂ x Mp*coi1-1* ♀, Mp*coi1-2* ♂ x Tak-2 ♀, and Mp*coi1-2* ♂ x Mp*coi1-1* ♀. (n=15 archegoniophores per genotype). Scale bar, 1 cm. (**d**) Segregation of Mp*coi1-1* mutation after crossing parental lines Tak-1 ♂ x Tak-2 ♀, Tak□ ♂ x Mp*coi1-1* ♀, Mp*coi1-1* ♂ x Tak-2 ♀, and Mp*coi1-1* ♂ x Mp*coi1-1* ♀. (n=27 plants).

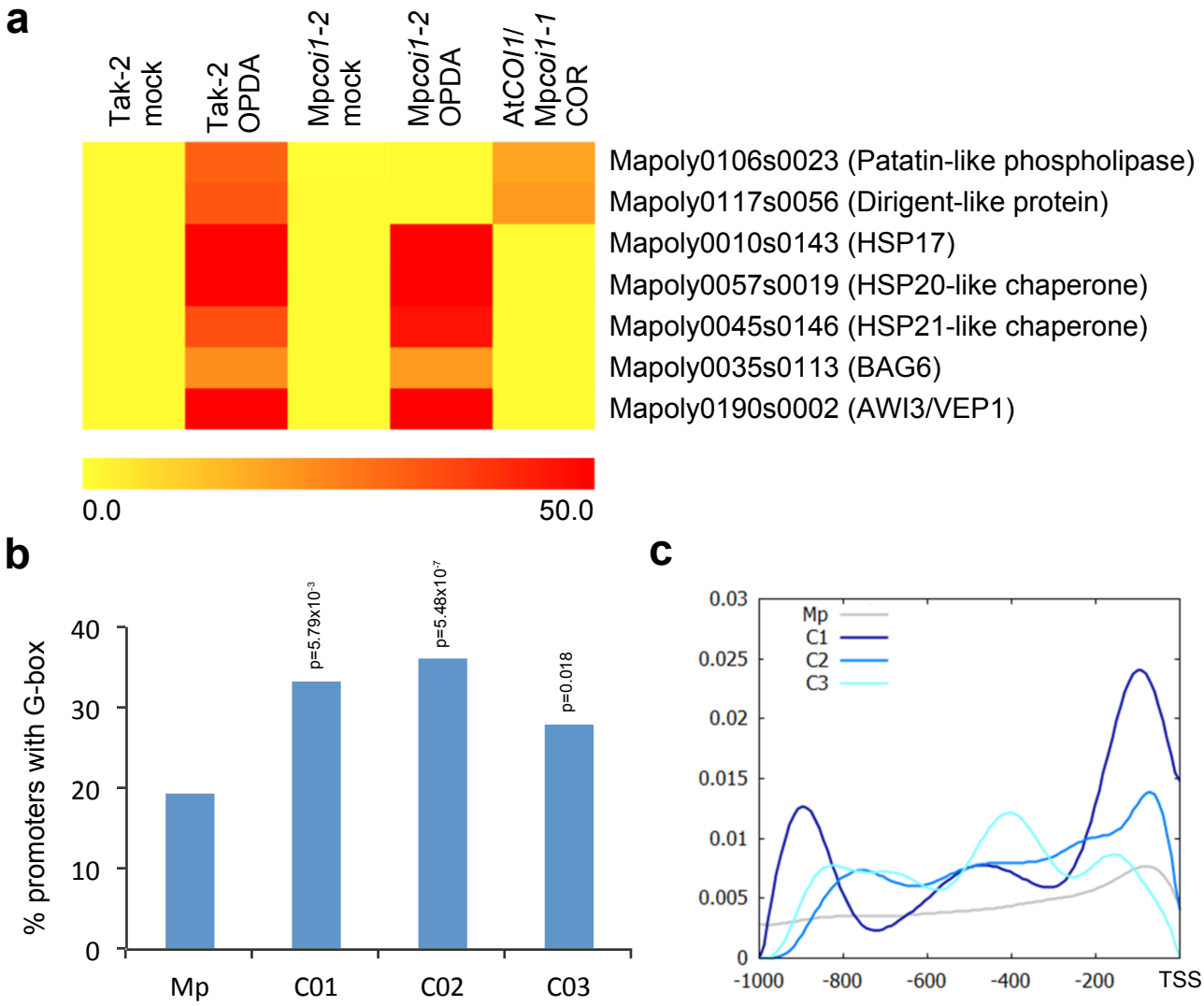

Supplementary Figure 3. (**a**) Expression analyses of OPDA-inducible genes by Q-PCR in WT Tak-2, and Mp*coi1-2* mutant treated or not with OPDA 25 μM for 2 h and complemented line At*COI1*/Mp*coi1-1* treated with COR 0.5 μM for 2 h. Data shown as mean of three independent biological replicates and three technical replicates. Color key shows relative expression levels referred to Tak-2 mock and using Mp*APT* as control gene. Gene codes are followed by the automatic annotation to indicate putative homologues. This experiment was repeated twice with similar results, (n=3 independent biological replicates formed by 11 plants each). (**b**) Over-representation of MYC-related transcription factors bound sequences in the promoters of OPDA/COI1 responding genes. Histogram with the percentage of promoter regions containing the G-box (CACGTG) in the complete set of Marchantia genes (Mp, n=19827 genes) and in the genes included in each of the clusters obtained in **Figure 3b** (C01, n=54 genes; C02, n=149 genes; C03, n=79 genes). Clusters 1 and 2 are particularly enriched in G-boxes. Asterisks indicate statistical significance between the proportions in each cluster and the proportion of the G-box in the complete set of Marchantia promoters. p-values were calculated with hypergeometric test. Promoter regions (1 kb upstream the annotated transcription start site) were obtained using BEDTOOLS[58] from the Marchantia genome sequence (Mpolymorpha_320_v3.0.fa) and the annotation file (Mpolymorpha_320_v3.1.gene.gff3), both downloaded from Phytozome. Sequence scan for the perfect G-box (CACGTG) in the complete set of promoters was performed with the "dna-pattern" tool in RSAT[59], that gives the coordinate position in the promoter sequence. (**c**) G-boxes are enriched in proximal promoters. Density plot (proportion of binding sites at each coordinate position) of the G-boxes found in promoter regions (1000 bp upstream the transcription start site, TSS) of the Marchantia genes (Mp) and of the genes included in each cluster. G-boxes are particularly enriched in the proximal promoters near the TSS of genes from clusters 1 and 2. Coordinate positions were obtained from sequence scan as in panel **b**, histograms scored at 10 bp intervals and plotted with 'gnuplot 4.6' (http://www.gnuplot.info/).

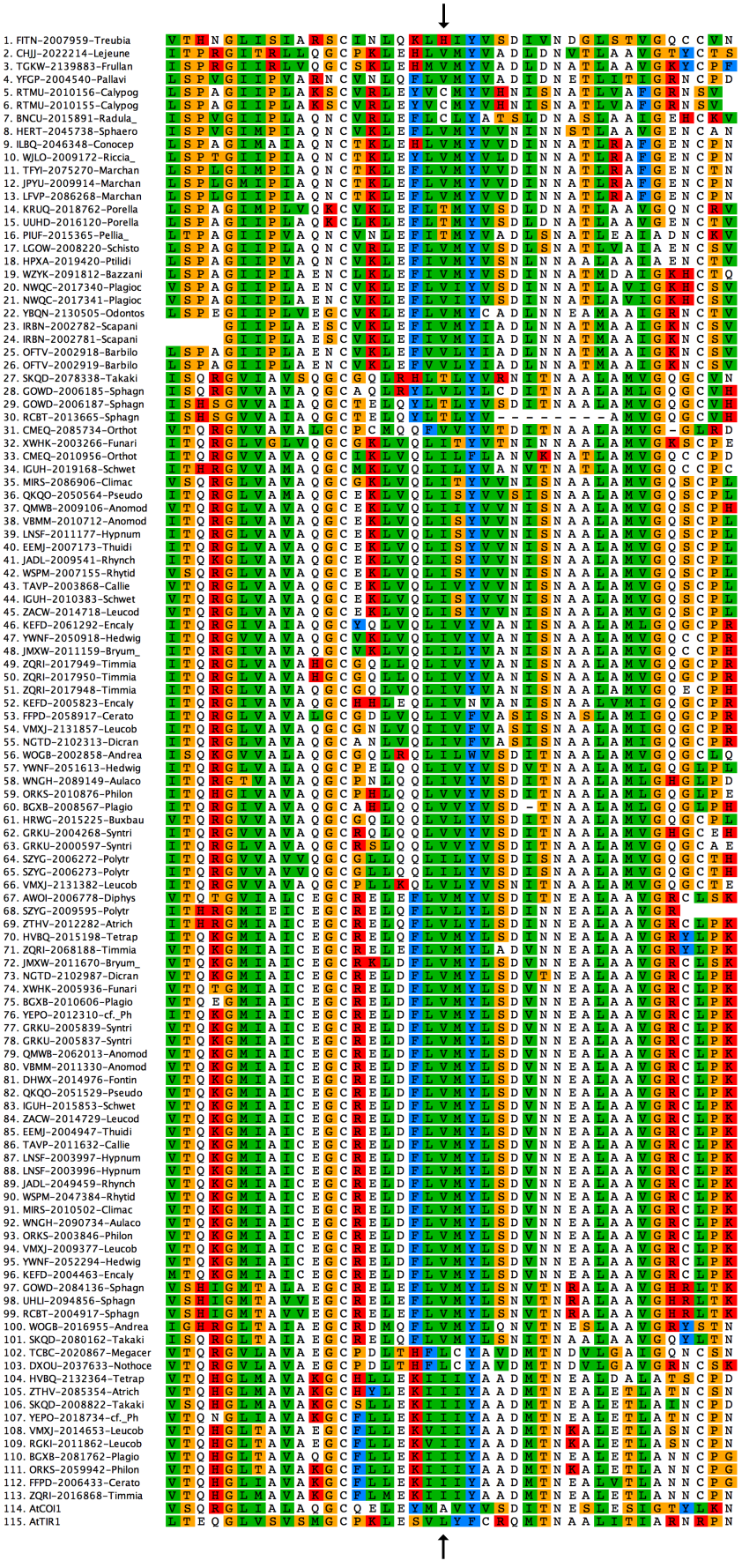

Supplementary Figure 4: No available bryophyte COI1 sequences have an alanine at the position equivalent to AtCOI1^{A384}. Multiple sequence alignment of the predicted bryophyte COI1 amino acid sequences from OneKP database (see reference 16 for full species name and corresponding codes). AtCOI1 and AtTIR1 sequences are included for comparison (bottom). Arrows indicate the position at which AtCOI1 has an alanine, whereas all bryophytes have a residue other than alanine.

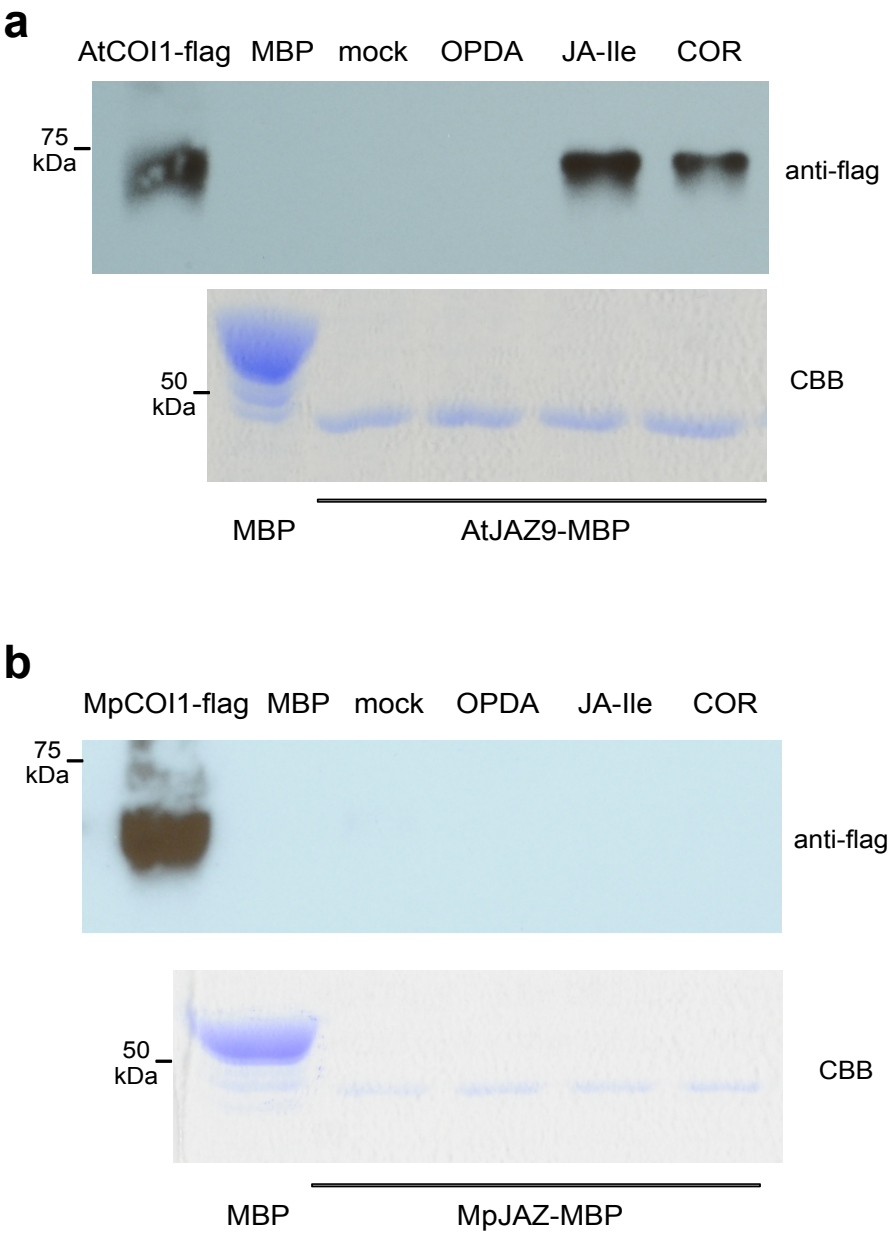

Supplementary Figure 5. The COI-JAZ co-receptor has distinct hormone specificities in *Arabidopsis* and *Marchantia*. (**a**) Immunoblot (anti-flag antibody) of recovered AtCOI1-flag (from 35S:At*COI1*-flag Arabidopsis extracts) after pull-down reactions using recombinant AtJAZ9-MBP protein alone (mock) or with different molecules: OPDA (50 μM), JA-Ile (50 μM), COR (0.5 μM). Bottom, Coomassie blue staining of AtJAZ9-MBP after Factor Xa cleavage. This experiment was repeated 5 times with similar results. (**b**) Immunoblot of MpCOI1-flag (from 35S:Mp*COI1*-flag Arabidopsis extracts) after pull-down reactions using recombinant MpJAZ-MBP protein alone (mock) or with OPDA (50 μM), JA-Ile (50 μM) and COR (0.5 μM). Bottom, Coomassie blue staining of MpJAZ-MBP after Factor Xa cleavage. This experiment was repeated 5 times with similar results. Uncropped blots are shown in **Supplementary Fig. 10c,d**.

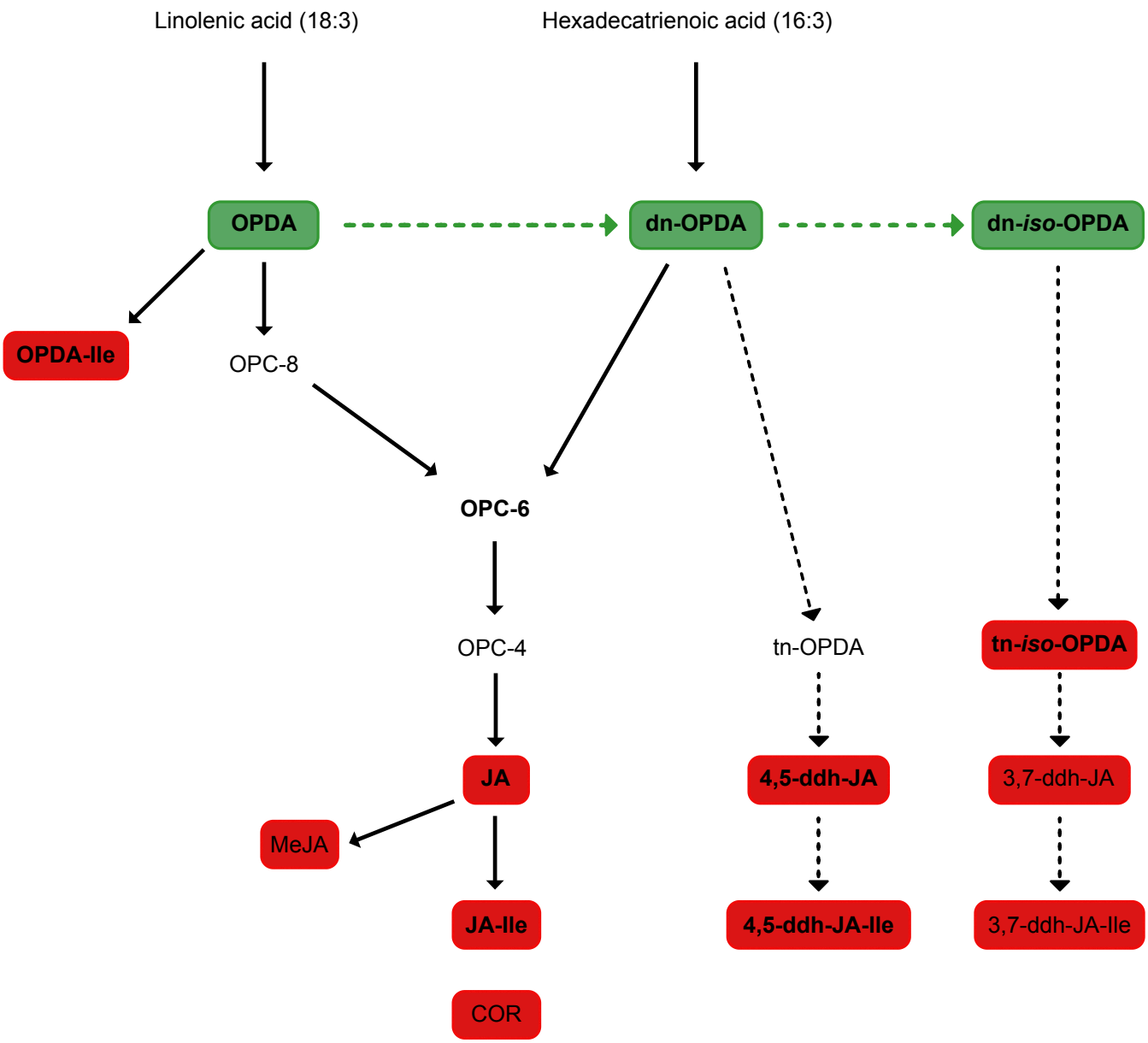

Supplementary Figure 6. Biosynthetic pathways of JA-Ile and related oxylipins. Black arrows indicate steps described in tracheophytes. Black dashed lines indicate hypothetic alternative reactions not yet described in plants. Red indicates inactive molecules that do not inhibit growth in *M. polymorpha*, green indicates active molecules that inhibit growth in *M. polymorpha* (OPDA, dn-OPDA and dn-*iso*-OPDA). Green dashed line indicates the OPDA-to-dinor-OPDA-to-dinor-*iso*-OPDA conversion in *M. polymorpha* described in this study. Bold letters indicate molecules used as internal standards in *M. polymorpha* (OPDA, dn-OPDA, OPDA-Ile, OPC-6, JA, JA-Ile, 4,5-ddh-JA, 4,5-ddh-JA-Ile and tetranor-*iso*-OPDA).

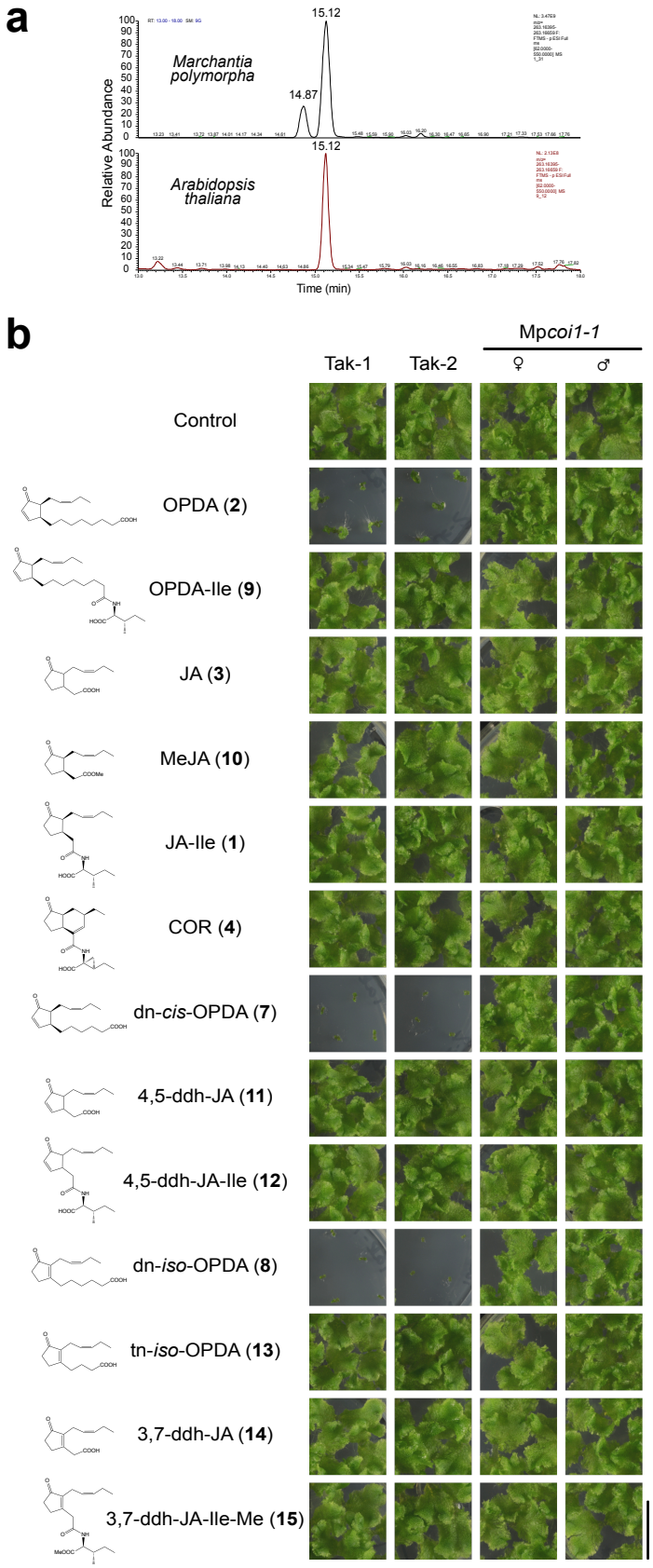

Supplementary Figure 7. Only OPDA, dinor-*cis*-OPDA and dinor-*iso*-OPDA inhibit growth in *M. polymorpha* and this inhibition is Mp*COI1*-dependent. (**a**) Chromatogram of dinor-OPDA (15.12) and dinor-*iso*-OPDA (14.87) in wounded *M. polymorpha* and *A. thaliana*. This experiment was repeated three times with similar results, (n=4 independent biological replicates of 8 plants each). (**b**) Effect of various oxylipins [OPDA (**2**), OPDA-Ile (**9**), JA (**3**), MeJA (**10**), JA-Ile (**1**), dinor-*cis*-OPDA (**7**), 4,5-ddh-JA (**11**), 4,5-ddh-JA-Ile (**12**), dinor-*iso*-OPDA (**8**), tetranor-*iso*-OPDA (**13**), 3,7-ddh-JA (**14**) and 3,7-ddh-JA-Ile-Me (**15**); all 50 μM] and coronatine (**4**; 0.5 μM) on 19-day-old *M. polymorpha* WT Tak-1 and Tak-2 and Mp*coi1-1* male and female mutants. This experiment was repeated 3 times with similar results, (n=8 plants). Scale bar, 1 cm.

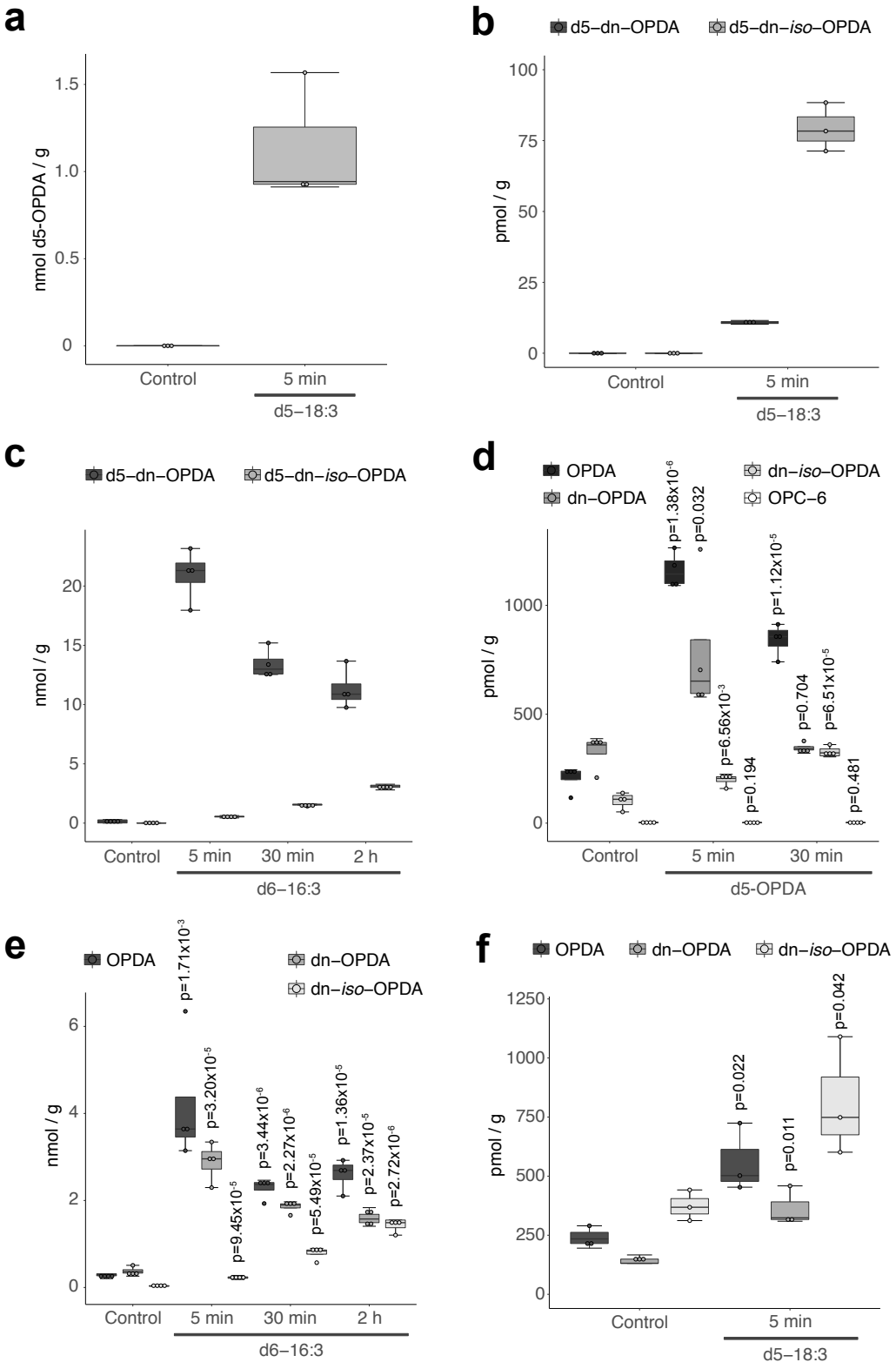

Supplementary Figure 8. 16:3 and 18:3 are dn-OPDA precursors and the oxylipin biosynthesis feedback loop is conserved in *M. polymorpha*. (**a**) Accumulation of deuterated OPDA (d5-OPDA) in Tak-1 upon 5 min treatment with deuterated linolenic acid (d5-18:3). (**b**) Accumulation of d5-dinor-OPDA and d5-dinor-*iso*-OPDA in Tak-1 after 5 min d5-18:3 treatment. (**c**) Accumulation of d5-dinor-OPDA and d5-dinor-*iso*-OPDA in Tak-1 after treatment with deuterated hexadecatrienoic acid (d6-16:3) for 5 min, 30 min and 2 h. (**d**) Accumulation of non-deuterated OPDA, dinor-OPDA, dinor-*iso*-OPDA and OPC-6 in Tak-1 plants in basal conditions and 5 or 30 min after d5-OPDA treatment. (**e**) Accumulation of non-deuterated OPDA, dinor-OPDA and dinor-*iso*-OPDA in Tak-1 plants in basal conditions and 5 min, 30 min and 2 h after treatment with d6-16:3. (**f**) Accumulation of non-deuterated OPDA, dinor-OPDA and dinor-*iso*-OPDA in Tak-1 plants in basal conditions and 5 min after treatment with d5-18:3. All panels, center lines are medians, boxes show the upper and lower quartiles and whiskers show the full data range except the outliers. Dots are individual data points (**a**, **b** and **f**, n=3 independent biological replicates of 11 plants each; **c**, **d** and **e**, n=4 independent biological replicates of 11 plants each). p-values in **d**, **e** and **f** were calculated with two-tailed Student's t-test.

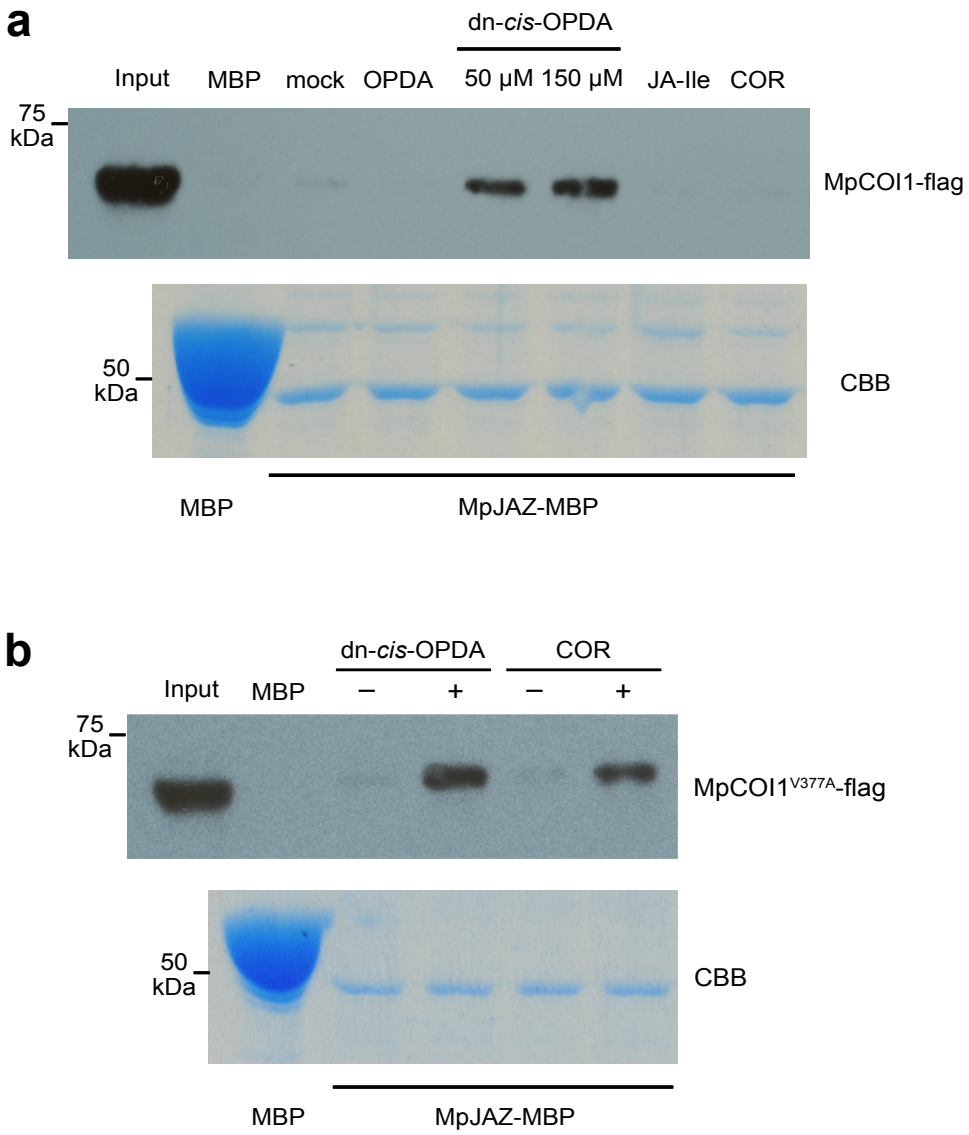

Supplementary Figure 9. The dinor-OPDA ligand binds to MpCOI1/MpJAZ and the point mutation MpCOI1^{V377A} perceives dn-OPDA and COR. (**a**) Immunoblot (anti-flag antibody) of recovered MpCOI1-flag (from 35S:Mp*COI1*-flag Arabidopsis extracts) after pull-down reactions using recombinant MpJAZ-MBP protein alone or with OPDA (50 μM), dinor-*cis*-OPDA (50 and 150 μM), JA-Ile (50 μM) and COR (0.5 μM). Bottom, Coomassie blue staining of MpJAZ-MBP after Factor Xa cleavage. This experiment was repeated 5 times with similar results. (**b**) Immunoblot (anti-flag antibody) of recovered MpCOI1^{V377A}-flag (from 35S:Mp*COI1*^{V377A}-flag Arabidopsis extracts) after pull-down reactions using recombinant MpJAZ-MBP protein alone (–) or with dinor-*cis*-OPDA (50 μM) or COR (0.5 μM). Bottom, Coomassie blue staining of MpJAZ-MBP after Factor Xa cleavage. This experiment was repeated 4 times with similar results. Uncropped blots are shown in **Supplementary Fig. 10e,f**.

a

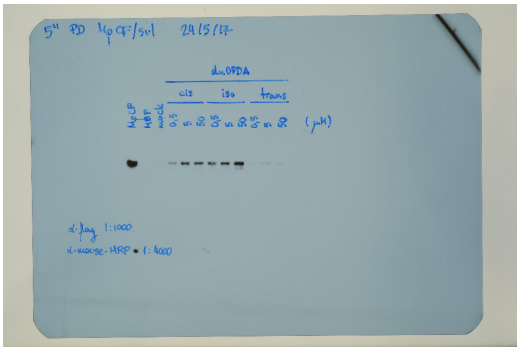

b

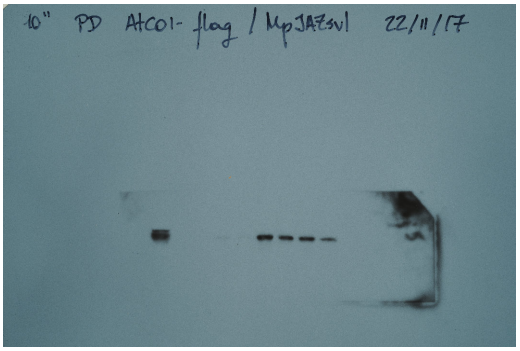

c

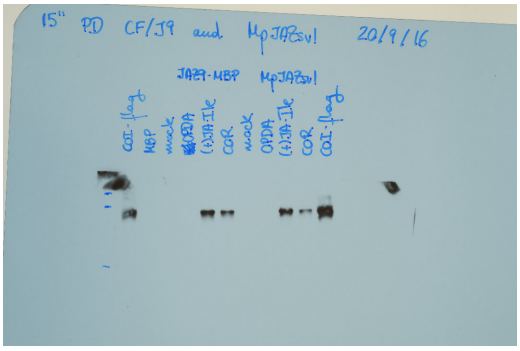

d

e

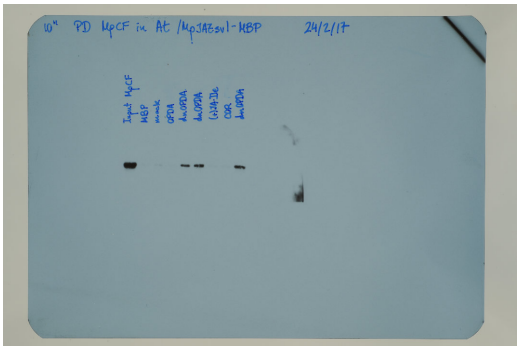

f

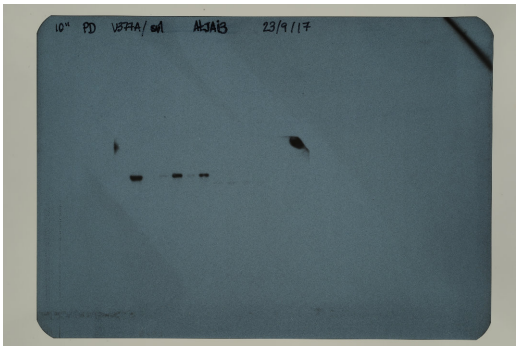

Supplementary Figure 10. Uncropped blots. (**a**) Full Western blot shown in **Fig. 6d**. (**b**) Full Western blot shown in **Fig. 6f**. (**c**) Full Western blot shown in **Supplementary Fig. 5a**. (**d**) Full Western blot shown in **Supplementary Fig. 5b**. (**e**) Full Western blot shown in **Supplementary Fig. 9a**. (**f**) Full Western blot shown in **Supplementary Fig. 9b**.

Supplementary Table 1: Primers

Primer name	Sequence
attB1 MpCOI1	GGGGACAAGTTTGTACAAAAAAGCAGGCTCCATGGAGGTGAGGGGTCCGGCCG
attB2 MpCOI1	GGGGACCACTTTGTACAAGAAAGCTGGGTTTCATAGTTCCCAATTTTCCCGCGCTGG
attB2 no stop MpCOI1	GGGGACCACTTTGTACAAGAAAGCTGGGTATAGTTCCCAATTTTCCCGCGCTGGTG
attB1 MpJAZ	GGGGACAAGTTTGTACAAAAAAGCAGGCTCCATGCATCGCAATACTTGGAATAAGCC
attB2 MpJAZ	GGGGACCACTTTGTACAAGAAAGCTGGGTTCTAATGCCGTTGTGAGGGTGAAC
attB2 no stop MpJAZ	GGGGACCACTTTGTACAAGAAAGCTGGGTAATGCCGTTGTGAGGGTGAACCAG
attB1 MpASK1	GGGGACAAGTTTGTACAAAAAAGCAGGC TAC ATGTCGAAAGAAACGAAAGTAAAG
attB2 MpASK1	GGGG AC CAC TTT GTA CAA GAA AGC TGG GTG TCATTCGAAAGCCCACTGGTT
MpCOI1 Fwd PacI HR	ctaaggtagcgattaTTTGAATTCCGTGCTCTCCA
MpCOI1 Rev PacI HR	gcccgggcaagcttaACCCGAGTGTCTCATCCG
MpCOI1 Fwd AscI HR	taaactagtggcgcgTGCATGTTACCGATGCT
MpCOI1 Rev AscI HR	ttatccctaggcgcgTTAGTACCACAACCTATATA
COI1 Rv MpCOI1 tail	TGTATTATTGAGAGCAAGCTCATGAAGCCACTTACCAT
MpCOI1 Fw COI1 tail	GGTAAGTGGCTTCATGAGCTTGCTCTCAATAATACAACGTTG
MpCOI1 Rv COI1 tail	TGTGTTGTGCTGAGC*C*AGCTCATGTAACCATTCACCGCC
COI1 Fw MpCOI1 tail	GGTGAATGGTTACATGAGCT*G*GCTCAGCACAACACATC
MpCOI1 V377A Rev	ATGTCCACAACATACATCGCAAGAAACTCGAG
MpCOI1 V377A Fw	GCTCGAGTTTCTTGCGATGTATGTTGTGGAC
qPCR MpACT Fw	AGGCATCTGGTATCCACGAG
qPCR MpACT Rv	ACATGGTCGTTCCTCCAGAC
qPCR MpCOI1 1ex Fw	TCACTGAAGATTAAGGGCAAGCC
qPCR MpCOI1 1ex Rv	AACGAGCAGCTCATACTCGAAAG
MpCOI a	AGGACAGAAGGCACTGAAGTTC
MpCOI b	CTGCTTCTCAGAAACAGTCATGC
Primer X (MpEF_GT_R1)	GAAGGCTTCTGATTGAAGTTTCCTTTTCTG
gRNA1 MpCOI1 Fw	CTCGGCGACGATATGATGTGCTGC
gRNA1 MpCOI1 Rv	AAACGCAGCACATCATATCGTCGC
gRNA2 MpCOI1 Fw	CTCGGCCGAAGAAGTGACGACAGA
gRNA2 MpCOI1 Rv	AAACTCTGTCGTCACTTCTTCGGC
gRNA3 MpCOI1 Fw	CTCGTGTCAGTGTTGAAACTACAG
gRNA3 MpCOI1 Rv	AAACCTGTAGTTTCAACACTGACA
gRNA4 MpCOI1 Fw	CTCGGATTATGGTTCTTGTCATTC
gRNA4 MpCOI1 Rv	AAACGAATGACAAGAACCATAATC
Fw genotype Mpcoi	GGCAGGCACACAGACACTTA
Rv genotype Mpcoi	CAAGAGCACGAAGTCAACCA
MpAPT Q-PCR Fw	CGAAAGCCCAAGAAGCTACC
MpAPT Q-PCR Rv	GTACCCCCGGTTGCAATAAG
106s23 Fw qPCR	GAGATTCACCCCACAAAGAACG
106s23 Rv qPCR	GATCTTGGTAACCCTTGAAGTTGG
117s56 Fw qPCR	CGGAGAAGGTAATTGTCACCACA
117s56 Rv qPCR	TCTACCATACAGAGGACGTGATCG
10s143 Fw qPCR	TCGAAGGATGAGGCCAAGTTTC
10s143 Rv qPCR	GAACTTTCCAGCAGGTCTTTCCAT
35s113 Fw qPCR	CTACGTCCATCGAATCTGCTGAGT
35s113 Rv qPCR	TGGGATAAAAATCAACATCTCTCG
45s146 Fw qPCR	CATGTCTGCCTATTAGGAGGTCAC
45s146 Rv qPCR	CATTAGCAGTGTTTGATCCAAGG
57s19 Fw qPCR	CAGATCTTCCTGGCATGAAGAAAG
57s19 Rv qPCR	TGTCTGCCACTTGAATCTTAATCTC
190s2 Fw qPCR	GCCAGAATTTCTACTACACCTTGG
190s2 Rv qPCR	GCTTGAGGTGGTTGAACACAATAT

Supplementary Table 2: Ionization source working parameters

Instrumental parameters	**Value**
Sheath gas flow rate	44 au
Auxiliary gas flow rate	11 au
Sweep gas flow rate	1 au
Spray voltage	3.5 kV
Capillary temperature	340 ºC
S-lens RF level	50
Auxiliary gas heater temperature	300 ºC

Supplementary Dataset 1. Relative expression values (Log2 ratio) of the genes included in the clustering analysis shown in Figure 3b

Supplementary Dataset 2. Enriched Gene Ontology (GO) terms based on Marchantia annotations of the gene clusters shown in Figure 3b

Supplementary Dataset 3. Enriched Gene Ontology (GO) terms based on the Arabidopsis orthologues of genes shown in clusters in Figure 3b